

Non-affine deformation of semiflexible polymer networks

Sihan Chen^{1,2}, Tomer Markovich², Fred C. MacKintosh^{1,2,3,4}

¹*Department of Physics and Astronomy, Rice University, Houston, TX 77005*

²*Center for Theoretical Biological Physics, Rice University, Houston, TX 77005*

³*Department of Chemical and Biomolecular Engineering, Rice University, Houston, TX 77005*

⁴*Department of Chemistry, Rice University, Houston, TX 77005*

Networks of semiflexible or stiff polymers such as most biopolymers are known to deform inhomogeneously when sheared. The effects of such non-affine deformation have been shown to be much stronger than for flexible polymers. To date, our understanding of non-affinity in semiflexible systems is most limited to simulations or specific 2D models. Here, we present an effective medium theory (EMT) for non-affine deformation of semiflexible polymer networks, which is general to both 2D and 3D and in both thermal and athermal limits. The predictions of this model are in good agreement with both prior computational and experimental results for linear elasticity. Moreover, the framework we introduce can be extended to address nonlinear elasticity and network dynamics.

Networks of stiff or semiflexible polymers are vital for the function of most living systems. Such networks control much of the elastic properties of biomaterials ranging from the cell cytoskeleton to extra cellular matrices at the tissue scale [1–4]. Over the past few decades there was significant progress in our understanding the fundamental physical properties of semiflexible networks [5–16]. Previous studies of 2D and 3D semiflexible networks have, among other things, revealed a transition from bend-dominated, non-affine regime to a stretch-dominated, affine regime [17–26] that is governed by the average polymer length (or molecular weight), in stark contrast with flexible polymer systems.

The classical theory of *rubber elasticity* [27–29] is very successful in describing the elastic properties of flexible polymers networks. Early approaches assumed deformations to be affine, such that the strain tensor is microscopically uniform and independent of local structure. The phantom-network model relaxed the affine assumption and showed that local network structure indeed affects elastic properties, but in a way that does not change the basic scaling with macroscopic quantities such as average polymer length, system volume, temperature, etc. [30]. Unlike their flexible counterparts, the strong bending rigidity of individual semiflexible polymers leads to much stronger non-affine effects [17, 18, 31], and even give rise to a surprising dependence on dimensionality [20]. Most of the prior work accounting for non-affinity in semiflexible networks has been limited to numerical simulation [32–35], while a theory analogous to the phantom network has been lacking, especially in 3D. The strong bending interactions between sequential polymer segments along a chain precludes a direct application of phantom network-like models. Various models based on effective medium theories (EMT) introduced for rigidity percolation [36–38] have been proposed for lattice-based or topologically similar networks [19, 22, 39–43], along with floppy mode models for off-lattice networks [44, 45]. But, both of these approaches have been limited to 2D and quantitative agreement with simulation is still lim-

ited.

Here, we develop an analytical model for the non-affine deformation of semiflexible polymer networks. Our model applies to both lattice-based and random, off-lattice networks that are isotropic and homogeneous on large scales. As we show, this model can be applied to both thermal and athermal limits. Our prediction of the bend-to-stretch transition quantitatively agrees with previous simulations on 3D networks, while explaining the different scaling dependences on filament length in 2D lattice and off-lattice (e.g., Mikado) networks as well. Moreover, this model predicts a bend-to-stretch transition for thermal networks that agrees with previous experiments [24, 46]. While we focus here on the linear elastic limit, this model can also be extended to address the role of non-affine fluctuations in the dynamics [47–50], stress-stiffening [10, 11] and recently identified strain-controlled criticality [51–54].

We begin by considering an athermal crosslinked semiflexible polymer network in 3D. The discussion on 2D and thermal networks is postponed to later. The network is formed by N filaments each with polymer length L and average crosslinking distance ℓ_c . Its Hamiltonian is:

$$H_O = \sum_{\alpha=1}^N \left[H_b [\mathbf{u}^\alpha(s)] + H_s [\mathbf{u}^\alpha(s)] \right], \quad (1)$$

where $\mathbf{u}^\alpha(s) = \mathbf{u}_\parallel^\alpha(s) + \mathbf{u}_\perp^\alpha(s)$ is the microscopic displacement of the α -th polymer at position s along its contour length ($-L/2 < s < L/2$), with $\mathbf{u}_\parallel^\alpha(s)$ and $\mathbf{u}_\perp^\alpha(s)$ being its longitudinal and transverse components, respectively. $H_b [\mathbf{u}(s)] = \kappa \int ds |\partial^2 \mathbf{u}_\perp / \partial s^2|^2 / 2$ and $H_s [\mathbf{u}(s)] = \mu \int ds |\partial \mathbf{u}_\parallel / \partial s|^2 / 2$ are the bending and stretching energy, respectively. If a crosslink exists between the α -th and the β -th polymer, it leads to an additional constraint, $\mathbf{u}^\alpha(s_{\alpha\beta}) = \mathbf{u}^\beta(s_{\beta\alpha})$, with $s_{\alpha\beta}$ ($s_{\beta\alpha}$) being the position of the crosslink on the α -th (β -th) polymer.

We are interested in how this network deforms under an external shear stress σ_O . For athermal networks the deformation is found from the minimum-energy state,

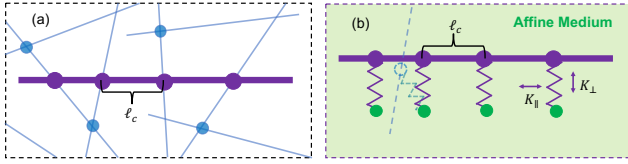


Figure 1. (a) 2D sketch of a crosslinked semiflexible polymer network, with average crosslinking distance ℓ_c . (b) Sketch of the EMN, in which crosslinks are replaced by springs that connects the polymers with a medium which deforms affinely (two polymers connected by one crosslinker are connected to the medium via two different springs). Spring constants for the parallel and transverse directions of the connected polymer are K_{\parallel} and K_{\perp} , respectively.

in which the microscopic deformations of each polymer are denoted by $\tilde{\mathbf{u}}^{\alpha}(s)$ and the shear strain of the entire network is γ_O . The linear shear modulus is defined as $G_O = \partial\sigma_O/\partial\gamma_O|_{\gamma_O=0}$. For simplicity we assume a stress σ_O in the $x-z$ plane. This causes (in the linear regime) a simple shear of the $x-z$ plane in the x direction, such that γ_O corresponds to a single nonzero term $\Lambda_{xz} = \gamma_O$ in the deformation tensor $\underline{\Lambda}$.

Although the network Hamiltonian has a quadratic form (Eq. (1)), a direct analytical solution of the minimum-energy state is challenging for two reasons: the first is the existence of the crosslinking constraints, which introduces correlations between different polymers. Therefore, their deformations $\mathbf{u}^{\alpha}(s)$ can not be considered as independent variables; the other is the unclear relation between the microscopic deformations (\mathbf{u}^{α}) and the macroscopic deformation (γ_O) for non-affine deformations. Below we detail how we overcome these challenges.

To remove the crosslink constraints, we have developed an EMN, in which all the polymers in the original network are preserved while all crosslinks are removed. To mimic the restraining effect of the crosslinks, each crosslink is replaced by a spring that connects the polymer at the position of the crosslink, with an effective medium. The medium deforms affinely and each spring has two spring constants, K_{\parallel} and K_{\perp} , for the parallel and transverse direction of its connected polymer, respectively. The resulting EMN has an additional elastic energy H_K and the effective Hamiltonian is

$$H_{\text{EM}} = \sum_{\alpha=1}^N \left(H_b[\mathbf{v}^{\alpha}(s)] + H_s[\mathbf{v}^{\alpha}(s)] + H_K[\mathbf{v}_{\text{NA}}^{\alpha}(s)] \right), \quad (2)$$

where the microscopic deformation in the EMN is denoted by $\mathbf{v}^{\alpha}(s) = \mathbf{v}_A^{\alpha}(s) + \mathbf{v}_{\text{NA}}^{\alpha}(s)$, with $\mathbf{v}_A^{\alpha}(s)$ being the affine displacement and $\mathbf{v}_{\text{NA}}^{\alpha}(s)$ being the non-affine displacement. Note that only non-affine displacements affect H_K , since forces are induced between affinely deforming polymers that simply stretch/compress uni-

formly. The microscopic affine displacements are given by $\mathbf{v}_A^{\alpha}(s) = s \underline{\Lambda} \cdot \hat{\mathbf{n}}^{\alpha}$, with $\hat{\mathbf{n}}^{\alpha}$ defining the polymer orientation. The additional energy H_K is the summation of the elastic energy of all springs connected to each polymer:

$$H_K[\mathbf{v}_{\text{NA}}^{\alpha}(s)] = \frac{K_{\parallel}}{2} \sum_i |\mathbf{v}_{\text{NA}\parallel}^{\alpha}(s_i)|^2 + \frac{K_{\perp}}{2} \sum_i |\mathbf{v}_{\text{NA}\perp}^{\alpha}(s_i)|^2, \quad (3)$$

where s_i is the position of the i -th spring, and $v_{\text{NA}\perp}^{\alpha}$ and $v_{\text{NA}\parallel}^{\alpha}$ are the transverse and longitudinal components of $\mathbf{v}_{\text{NA}}^{\alpha}$, respectively. Importantly, Eq. (2) describes a single-polymer Hamiltonian in which the network structure is accounted for through a harmonic energy. Such approach is conceptually similar to the effective spring constant introduced in Refs. [55, 56] for entangled polymer solutions.

Under an imposed shear stress σ_{EM} , we define the microscopic deformations in the minimum-energy state are $\tilde{\mathbf{v}}^{\alpha}(s)$, with a shear strain γ_{EM} and an elastic modulus $G_{\text{EM}} = \partial\sigma_{\text{EM}}/\partial\gamma_{\text{EM}}|_{\gamma_{\text{EM}}=0}$. Our goal is to find an EMN that reproduces the elasticity of the original network, i.e. $G_{\text{EM}} = G_O$, the inverse of which can be rewritten using the chain rule:

$$\sum_{\alpha i} \frac{\partial \tilde{\mathbf{u}}_i^{\alpha}}{\partial \sigma_O} \cdot \frac{\partial \gamma_O}{\partial \tilde{\mathbf{u}}_i^{\alpha}} = \sum_{\alpha i} \frac{\partial \tilde{\mathbf{v}}_i^{\alpha}}{\partial \sigma_{\text{EM}}} \cdot \frac{\partial \gamma_{\text{EM}}}{\partial \tilde{\mathbf{v}}_i^{\alpha}}, \quad (4)$$

where $\tilde{\mathbf{u}}_i^{\alpha} = \tilde{\mathbf{u}}^{\alpha}(s_i)$ and $\tilde{\mathbf{v}}_i^{\alpha} = \tilde{\mathbf{v}}^{\alpha}(s_i)$ are the displacements on the crosslink positions. To ensure that Eq. (4) is satisfied, we look for simultaneous solutions to

$$\left\langle \frac{\partial \tilde{\mathbf{u}}_i^{\alpha}}{\partial \sigma_O} \right\rangle = \frac{\partial \tilde{\mathbf{v}}_i^{\alpha}}{\partial \sigma_{\text{EM}}} \quad (5a)$$

$$\frac{\partial \gamma_O}{\partial \tilde{\mathbf{u}}_i^{\alpha}} = \frac{\partial \gamma_{\text{EM}}}{\partial \tilde{\mathbf{v}}_i^{\alpha}}. \quad (5b)$$

In Eq. (5a) we average the effects of random crosslinking angles in the original network. These requirements may not be the only appropriate ones and may appear to be stronger than necessary. However, as we will show later, this choice does lead to good agreement with the expected macroscopic elasticity. Equation (5a) is essentially a coherent potential approximation (CPA) as in the classic EMT of 2D lattice-based networks [38, 57]. Importantly, Eq. (5b) is different from what is usually done in an EMT, in that it allows our EMN to deform non-affinely.

We start with the first requirement. Equation (5a) describes the local displacement caused by the stress, which can thus be considered as a local compliance. As the stress can be decomposed to local forces on each node in the network, we exert a test force \mathbf{F} on a particular node on the same polymer in both the original network and the EMN, and measure the resulting displacements, $\delta \mathbf{r}_O$ and $\delta \mathbf{r}_{\text{EM}}$ in two networks (see Fig. 2). By letting

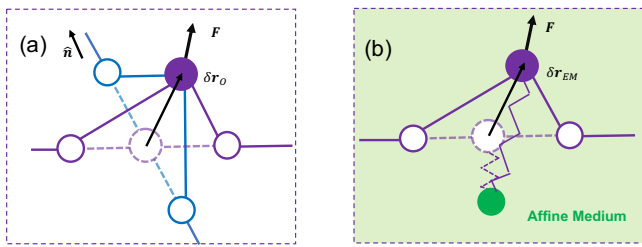


Figure 2. Sketch of the test force approach. A particular node on the purple polymer is deformed by a test force \mathbf{F} . The resulting displacement is $\delta\mathbf{r}_O$ in the original network (a), and $\delta\mathbf{r}_{EM}$ in the EMN (b).

$\langle\delta\mathbf{r}_O\rangle_{\hat{\mathbf{n}}} = \delta\mathbf{r}_{EM}$, where $\hat{\mathbf{n}}$ is the orientation of the other polymer crosslinked to the node in the original network, we obtain the values of the two spring constants, which for 3D networks read (see Sec. I of [57]):

$$K_{\perp} = K_{\parallel} = \frac{18\kappa}{\ell_c^3}. \quad (6)$$

The equality of K_{\perp} and K_{\parallel} is consistent with an isotropic effective medium. Importantly, however, the node compliance is still highly anisotropic due to H_s .

To solve Eq. (5b), one needs to find the relation between the macroscopic deformation $\underline{\underline{\mathbf{A}}}$ and the microscopic deformations \mathbf{u}^{α} . This is simple in the affine limit, as noted above. For non-affine deformations the situation is more complex. To address this, instead of determining \mathbf{u}^{α} from $\underline{\underline{\mathbf{A}}}$, we do it inversely by determining $\underline{\underline{\mathbf{A}}}$ from \mathbf{u}^{α} . We assume $\underline{\underline{\mathbf{A}}}$ to be a functional of all microscopic deformations, $\underline{\underline{\mathbf{A}}}[\mathbf{u}^1(s), \mathbf{u}^2(s), \dots, \mathbf{u}^N(s)]$. In the small strain limit, we can always perform a linear expansion,

$$\underline{\underline{\mathbf{A}}} = \sum_{\alpha} \int_{-L/2}^{L/2} ds \mathbf{u}^{\alpha}(s) \cdot \underline{\underline{\mathbf{T}}}^{\alpha}(s), \quad (7)$$

where $\underline{\underline{\mathbf{T}}}^{\alpha}(s)$ is a third-order coefficient tensor. We find that $\underline{\underline{\mathbf{T}}}^{\alpha}(s)$ can be uniquely determined from three conditions: (i) the affine deformation should satisfy Eq. (7), as it is a special case of the non-affine deformation; (ii) we assume the network is homogeneous on large scale, so all polymers are identical to each other except for their different orientations, leading to $\underline{\underline{\mathbf{T}}}^{\alpha}(s) = \underline{\underline{\mathbf{T}}}(\hat{\mathbf{n}}^{\alpha}, s)$; (iii) we assume the network is isotropic [58]. The full derivation of $\underline{\underline{\mathbf{T}}}$ is detailed in Sec. II of [57]. A similar macroscopic-microscopic relation can be defined for the EMN as well with a coefficient tensor $\underline{\underline{\mathbf{T}}}_{EM}^{\alpha}(s)$, whose value is related to $\underline{\underline{\mathbf{T}}}^{\alpha}(s)$ via Eq. (5b). For 3D networks $\underline{\underline{\mathbf{T}}}_{EM} = \underline{\underline{\mathbf{T}}}$, while for 2D networks $\underline{\underline{\mathbf{T}}}_{EM}$ becomes more complicated due to the *floppy mode* deformation [44], see discussion later.

By solving Eqs. (5a) and (5b), we have linked the EMN to the original network. The EMN elasticity G_{EM} can be found by minimizing Eq. (2) under an applied stress, which should be consistent with the elasticity of the original network G_O (see Sec. III A of Ref. [57] for more

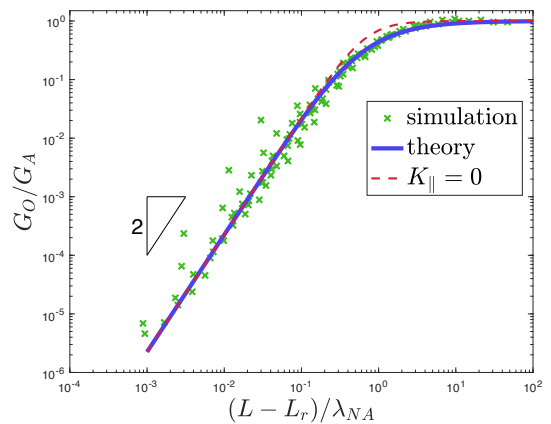


Figure 3. Shear modulus for 3D athermal networks. Simulation results of phantom-fcc-lattice network is reproduced from Ref. [20], with filament length corrected by the minimum length of rigidity percolation, $L_r = 2.85\ell_c$. Theoretical prediction is plotted using Eq. (S41) in Ref. [57], which is similar to Eq. (8) but calculated for networks with exponential length distribution as in the simulation.

detail). For 3D athermal monodispersed networks (all polymers have the same length) we find that

$$\frac{G_O}{G_A} = \left[1 + \frac{4\sqrt{2}\lambda_{NA}}{L} \cdot \coth\left(\frac{3L}{\sqrt{2}\lambda_{NA}}\right) \right]^{-1}, \quad (8)$$

where $G_A = \rho\mu/15$ is the affine linear elastic modulus, ρ is the polymer length density and $\lambda_{NA} = \ell_c^2/\sqrt{\kappa/\mu}$ is a characteristic non-affine lengthscale. We compare this theoretical prediction with previous simulations on lattice-based 3D networks [20] and find good quantitative agreement in both the scaling for small polymer length L ($G_O \sim L^2$) and in the transition to an affine deformation regime for larger L (Fig. 3). Interestingly, the non-affinity in the EMN is dominated by K_{\perp} over K_{\parallel} . For comparison we also plot in Fig. 3 the predicted modulus with $K_{\parallel} = 0$, showing a minor difference in the non-affine/affine transition region. This shows that the longitudinal deformation of the polymers is dominated by their own stretching rigidity, while K_{\parallel} has a minor effect, mainly in the non-affine/affine transition, where almost all longitudinal deformation is achieved from bending surrounding polymers. For simplicity we neglect K_{\parallel} hereafter.

Having demonstrated the elasticity of athermal networks, we consider thermal networks at finite temperature T , which results in fluctuations of the network state around the minimum-energy state. The elasticity can be found by calculating the average strain of the Boltzmann distribution (see Sec. III B of Ref. [57]),

$$G_O = \frac{\rho\mu_{ph}}{15} (1 + 266.7\ell_c\ell_p/L^2)^{-1}, \quad (9)$$

where $\ell_p = \kappa/(k_B T)$ is the persistence length, with k_B being the Boltzmann constant. Here $\mu_{ph} = 100\kappa\ell_p/\ell_c^3$

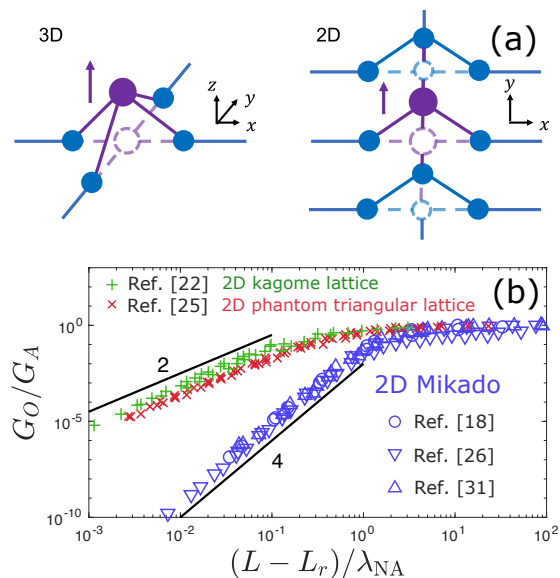


Figure 4. (a). Difference between 3D and 2D networks. In 3D networks, a crosslinker can deform in the direction perpendicular to its two connected polymers, without deforming other crosslinkers. In 2D networks, an entire polymer has to move together with the crosslinker, leading to deformation of L/ℓ_c crosslinkers. (b). Scaling dependence in 2D Mikado and 2D lattice networks. $\lambda_{NA} = \kappa^{-1/4} \mu^{1/4} \ell_c^{3/2}$ for Mikado and $\lambda_{NA} = \kappa^{-1/2} \mu^{1/2} \ell_c^2$ for lattice. $L_r = 5.9\ell_c$ (Mikado), $2.94\ell_c$ (phantom triangular) and $2.53\ell_c$ (kagome) are the minimum lengths for rigidity percolation. Simulation data reproduced from Ref. [18, 26, 31] (Mikado), Ref. [22] (kagome lattice) and Ref. [25] (phantom triangular lattice). The divergence between Ref. [22] and Ref. [25] is due to their different lattice structures.

is the effective stretch rigidity in the presence of thermal fluctuations. Interestingly, the limit $L \rightarrow \infty$ corresponds to a high molecular-weight analog of a phantom network, including node fluctuations. This slightly differs ($\sim 10\%$) from the limit of affinely deforming nodes with only transverse bending fluctuations [5, 11, 57].

Above we have focused on 3D networks, but our theory is general to other dimensionalities. There is, however, an essential difference between 3D and 2D networks, due to the Maxwell isostatic condition for rigidity percolation for coordination number $z = Z_c = 2d$ in dimension d . For networks formed by long polymers the connectivity approaches 4 from below. The local, near isostatic connectivity in 2D leads to long-range floppy modes [44, 45] that are absent in 3D, for which there is always a local floppy mode (see Fig. 4(a)). In 2D networks, independent displacements of crosslinks are prohibited without stretching. In the limit of large μ , when one crosslink in a 2D network is displaced, all other crosslinks on its connected polymer must be deformed in a particular way to avoid stretching deformation (see Fig. 4(b)), leading to L/ℓ_c crosslinks that displace together. The *floppy-mode* deformation requires us to take into account the

coupled deformation of multiple crosslinkers when calculating both the medium rigidity (Eq. (6)) and the coefficient tensor (Eq. (7)). Here, $K_{\perp} \sim L$ for a 2D lattice. For Mikado networks, K_{\perp} is further enhanced by the broad distribution of crosslink separations ℓ_c along the backbone [44], resulting in $K_{\perp} \sim L^3$. As shown in Sec. IV of [57], we predict the following scaling dependences in the non-affine regime:

$$G_O \sim \begin{cases} L^2 & (3D, \text{any structure}) \\ L^2 & (2D, \text{lattice}) \\ L^4 & (2D, \text{Mikado}) \end{cases} \quad (10)$$

Equation (10) agrees with previous numerical studies for 3D lattices [20], 2D lattices [22, 25], and 2D Mikado networks [17, 18, 23, 26, 31], as shown in Fig. 4(b). While various molecular weight scalings of 2D Mikado networks have been reported, the previous numerical studies are consistent with a common $(L - L_r)^4$ (see Sec. IV of [57]). Interestingly, although the local network structure strongly affects the scaling dependence of 2D networks with different distributions of ℓ_c , our model predicts a L^2 scaling that is robust for any structure, including potentially broad, randomly distributed ℓ_c in experimentally relevant 3D networks. Previous experimental studies on hydrogels are consistent with an L^2 dependence in 3D [24, 46].

Conclusions- The model presented above constitutes a basis for understanding the linear elasticity of both thermal semiflexible polymer and athermal fiber networks in 2D and 3D, including non-affine effects. Such non-affine effects are known to be more important for such systems than for flexible polymer gels, although most prior work addressing non-affinity in such systems has been limited to simulation, particularly for 3D. Our EMN approach provides is in very good agreement with prior numerical simulations for athermal networks. Our model also identifies an important difference between 2D and 3D systems, with a dramatic dependence on local structure in 2D that is absent in 3D networks.

An important feature of our theory is that the EMN is allowed to deform non-affinely, allowing us to more accurately capture non-affine deformations of real networks. This also allows us to predict non-affine fluctuations including thermal fluctuations, in contrast to prior effective medium approaches. Our model can be extended to predict nonlinear elastic effects such as stress-stiffening [10, 11]. This is possible even with our assumptions above of small displacements, in a way similar to prior theories of nonlinear semiflexible chain stretching [5, 11, 59]. Our model can also be extended to address strain-controlled criticality that has previously been identified computationally [60]. However, an important limitation of our approach is that it is a mean-field theory, and cannot be expected to predict anomalous critical exponents. Moreover, with the Hamiltonian in Eq. (2),

the derivation of network dynamics is also straightforward. Finally, our EMN approach is not limited to permanently-crosslinked networks, and can be applied also to transiently-crosslinked networks [61–63]. Interestingly, in Refs. [55, 56] an effective spring constant, which is conceptually similar to our effective medium rigidity, is estimated for a solution of entangled polymers. When combined with the present model, this suggests a possible model for entangled solutions.

Acknowledgments: This work was supported in part by the National Science Foundation Division of Materials Research (Grant No. DMR-1826623) and the National Science Foundation Center for Theoretical Biological Physics (Grant No. PHY-2019745).

-
- [1] D. Fletcher and R. Mullins, *Nature* **463**, 485 (2010), cited By 1470.
- [2] J. L. Shivers, J. Feng, A. S. G. van Oosten, H. Levine, P. A. Janmey, and F. C. MacKintosh, *Proc. Natl. Acad. Sci. U.S.A.* **117**, 21037 (2020).
- [3] A. S. van Oosten, X. Chen, L. Chin, K. Cruz, A. E. Patteson, K. Pogoda, V. B. Shenoy, and P. A. Janmey, *Nature* **573**, 96 (2019).
- [4] A. W. Hudnut, L. Lash-Rosenberg, A. Xin, J. A. Leal Doblado, C. Zurita-Lopez, Q. Wang, and A. M. Armani, *ACS Biomater. Sci. Eng.* **4**, 1916 (2018).
- [5] F. C. MacKintosh, J. Käs, and P. A. Janmey, *Phys. Rev. Lett.* **75**, 4425 (1995).
- [6] H. Isambert and A. Maggs, *Macromolecules* **29**, 1036 (1996).
- [7] K. Kroy and E. Frey, *Phys. Rev. Lett.* **77**, 306 (1996).
- [8] B. Hinner, M. Tempel, E. Sackmann, K. Kroy, and E. Frey, *Phys. Rev. Lett.* **81**, 2614 (1998).
- [9] D. C. Morse, *Macromolecules* **31**, 7030 (1998), cited By 177.
- [10] M. L. Gardel, J. H. Shin, F. C. MacKintosh, L. Mahadevan, P. Matsudaira, and D. A. Weitz, *Science* **304**, 1301 (2004).
- [11] C. Storm, J. J. Pastore, F. C. MacKintosh, T. C. Lubensky, and P. A. Janmey, *Nature* **435**, 191 (2005).
- [12] D. Mizuno, C. Tardin, C. F. Schmidt, and F. C. MacKintosh, *Science* **315**, 370 (2007).
- [13] O. Chaudhuri, S. H. Parekh, and D. A. Fletcher, *Nature* **445**, 295 (2007).
- [14] O. Stenull and T. Lubensky, arXiv preprint arXiv:1108.4328 (2011).
- [15] C. P. Broedersz and F. C. MacKintosh, *Rev. Mod. Phys.* **86**, 995 (2014).
- [16] R. H. Pritchard, Y. Y. S. Huang, and E. M. Terentjev, *Soft matter* **10**, 1864 (2014).
- [17] D. A. Head, A. J. Levine, and F. C. MacKintosh, *Phys. Rev. Lett.* **91**, 108102 (2003).
- [18] J. Wilhelm and E. Frey, *Phys. Rev. Lett.* **91**, 108103 (2003).
- [19] M. Das, F. C. MacKintosh, and A. J. Levine, *Phys. Rev. Lett.* **99**, 038101 (2007).
- [20] C. P. Broedersz, M. Sheinman, and F. C. MacKintosh, *Phys. Rev. Lett.* **108**, 078102 (2012).
- [21] A. Shahsavari and R. C. Picu, *Phys. Rev. E* **86**, 011923 (2012).
- [22] X. Mao, O. Stenull, and T. C. Lubensky, *Phys. Rev. E* **87**, 042602 (2013).
- [23] A. S. Shahsavari and R. C. Picu, *Int. J. Solids Struct.* **50**, 3332 (2013).
- [24] V. D. Nguyen, A. Pal, F. Snijkers, M. Colomb-Delsuc, G. Leonetti, S. Otto, and J. van der Gucht, *Soft Matter* **12**, 432 (2016).
- [25] A. J. Licup, A. Sharma, and F. C. MacKintosh, *Phys. Rev. E* **93**, 012407 (2016).
- [26] K. Baumgarten and B. P. Tighe, *Soft Matter* **17**, 10286 (2021).
- [27] M. Rubinstein and R. H. Colby, *Polymer Physics*, 1st ed. (Oxford, New York, 2003).
- [28] H. M. James, *J. Chem. Phys.* **15**, 651 (1947).
- [29] H. M. James and E. J. Guth, *J. Chem. Phys.* **11**, 455 (1948).
- [30] P. J. Flory, *Br. Polym. J.* **17**, 96 (1985).
- [31] D. A. Head, A. J. Levine, and F. C. MacKintosh, *Phys. Rev. E* **68**, 061907 (2003).
- [32] P. Onck, T. Koeman, T. Van Dillen, and E. van der Giessen, *Physical review letters* **95**, 178102 (2005).
- [33] J. S. Palmer and M. C. Boyce, *Acta biomaterialia* **4**, 597 (2008).
- [34] E. Huisman, C. Storm, and G. Barkema, *Physical Review E* **78**, 051801 (2008).
- [35] A. R. Cioroianu, E. M. Spiesz, and C. Storm, *Journal of the Mechanics and Physics of Solids* **89**, 110 (2016).
- [36] J. C. Phillips, *J. Non-Cryst. Solids* **34**, 153 (1979).
- [37] M. F. Thorpe, *J. Non-Cryst. Solids* **57**, 355 (1983).
- [38] S. Feng, M. F. Thorpe, and E. Garboczi, *Phys. Rev. B* **31**, 276 (1985).
- [39] C. P. Broedersz, X. Mao, T. C. Lubensky, and F. C. MacKintosh, *Nat. Phys.* **7**, 983 (2011).
- [40] M. Sheinman, C. P. Broedersz, and F. C. MacKintosh, *Phys. Rev. E* **85**, 021801 (2012).
- [41] X. Mao, O. Stenull, and T. C. Lubensky, *Phys. Rev. E* **87**, 042601 (2013).
- [42] J. Huang, J. O. Cochran, S. M. Fielding, M. C. Marchetti, and D. Bi, *Phys. Rev. Lett.* **128**, 178001 (2022).
- [43] O. K. Damavandi, M. L. Manning, and J. M. Schwarz, *EPL* **138**, 27001 (2022).
- [44] C. Heussinger and E. Frey, *Phys. Rev. Lett.* **97**, 105501 (2006).
- [45] D. Zhou, L. Zhang, and X. Mao, *Phys. Rev. Lett.* **120**, 068003 (2018).
- [46] M. Jaspers, M. Dennison, M. F. Mabeoone, F. C. MacKintosh, A. E. Rowan, and P. H. Kouwer, *Nat. Commun.* **5**, 1 (2014).
- [47] B. P. Tighe, *Phys. Rev. Lett.* **109**, 168303 (2012).
- [48] M. Yucht, M. Sheinman, and C. Broedersz, *Soft Matter* **9**, 7000 (2013).
- [49] R. Milkus and A. Zaccone, *Phys. Rev. E* **95**, 023001 (2017).
- [50] J. L. Shivers, A. Sharma, and F. C. MacKintosh, arXiv preprint arXiv:2203.04891 (2022).
- [51] A. Sharma, A. J. Licup, K. A. Jansen, R. Rens, M. Sheinman, G. H. Koenderink, and F. C. MacKintosh, *Nat. Phys.* **12**, 584 (2016).
- [52] M. F. J. Vermeulen, A. Bose, C. Storm, and W. G. Ellenbroek, *Phys. Rev. E* **96**, 053003 (2017).
- [53] M. Merkel, K. Baumgarten, B. P. Tighe, and M. L. Manning, *Proc. Natl. Acad. Sci. U.S.A.* **116**, 6560 (2019).

- [54] S. Arzash, J. L. Shivers, and F. C. MacKintosh, *Soft Matter* **16**, 6784 (2020).
- [55] D. C. Morse, *Phys. Rev. E* **63**, 031502 (2001).
- [56] H. Hirsch, J. Wilhelm, and E. Frey, *The European Physical Journal E* **24**, 35 (2007).
- [57] Supplementary material.
- [58] In principle the assumptions of homogeneity and isotropy are not required for the model. Here they are adopted for simplicity.
- [59] J. F. Marko and E. D. Siggia, *Macromolecules* **28**, 8759 (1995).
- [60] S. Chen, T. Markovich, and F. C. MacKintosh, unpublished.
- [61] O. Lieleg, M. M. A. E. Claessens, Y. Luan, and A. R. Bausch, *Phys. Rev. Lett.* **101**, 108101 (2008).
- [62] C. P. Broedersz, M. Depken, N. Y. Yao, M. R. Pollak, D. A. Weitz, and F. C. MacKintosh, *Phys. Rev. Lett.* **105**, 238101 (2010).
- [63] S. Chen, C. P. Broedersz, T. Markovich, and F. C. MacKintosh, *Phys. Rev. E* **104**, 034418 (2021).

Supplementary Material

I. DERIVATION OF THE MEDIUM RIGIDITY

A. Effective Spring Constants

In this section we derive the effective medium rigidity of a 3D network, *i.e.* the effective spring constants K_{\parallel} and K_{\perp} . As discussed in the main text, we exert a test force \mathbf{F} at a particular crosslinker on the same polymer, and calculate the resulting displacement, $\delta\mathbf{r}_O$ and $\delta\mathbf{r}_{EM}$ in both the original network and the effective medium network (EMN). By equating $\langle\delta\mathbf{r}_O\rangle_{\hat{\mathbf{n}}}$ and $\delta\mathbf{r}_{EM}$, where $\hat{\mathbf{n}}$ is the orientation of the other polymer crosslinked to the crosslinker in the original network, we find the values of K_{\parallel} and K_{\perp} . Below we detail the calculation.

We start with the EMN, whose Hamiltonian is described by Eq. (2) of the main text. Because we are mainly interested in the displacements of the crosslinkers (nodes connected to springs), we rewrite the bending and stretching energies of a particular polymer in a discrete form:

$$\begin{aligned}
 H_b[\mathbf{v}^\alpha(s)] &= \sum_i \frac{\kappa}{2\ell_c^3} |\mathbf{v}_\perp^\alpha(s_{i+1}) - 2\mathbf{v}_\perp^\alpha(s_i) + \mathbf{v}_\perp^\alpha(s_{i-1}))|^2 \\
 H_s[\mathbf{v}^\alpha(s)] &= \sum_i \frac{\mu}{2\ell_c} |\mathbf{v}_\parallel^\alpha(s_{i+1}) - \mathbf{v}_\parallel^\alpha(s_i)|^2
 \end{aligned} \tag{S1}$$

where $\mathbf{v}^\alpha(s_i)$ is the displacement of the i -th crosslinker and $\mathbf{v}_\parallel^\alpha(s_i)$ and $\mathbf{v}_\perp^\alpha(s_i)$ are its longitudinal and transverse components with respect to the polymer. We consider the case in which a particular crosslinker on this polymer deforms with displacement $\delta\mathbf{r}_{EM}$, while the positions of other crosslinkers are assumed to be fixed (such assumption is only appropriate for 3D networks, not for 2D networks, see Sec. IV), see Fig. S1 (a). The resulting energy is calculated from Eq. (S1):

$$\Delta H_{EM} = \Delta H_b(\delta\mathbf{r}_{EM\perp}) + \Delta H_s(\delta\mathbf{r}_{EM\parallel}) + \Delta H_K(\delta\mathbf{r}_{EM}) \tag{S2}$$

where $\Delta H_b(\delta\mathbf{r}_{EM\perp}) = (3\kappa/\ell_c^3)|\delta\mathbf{r}_{EM\perp}|^2$, $\Delta H_s(\delta\mathbf{r}_{EM\parallel}) = (\mu/\ell_c)|\delta\mathbf{r}_{EM\parallel}|^2$ and $\Delta H_K(\delta\mathbf{r}_{EM}) = (K_{\perp}/2)|\delta\mathbf{r}_{EM\perp}|^2 + (K_{\parallel}/2)|\delta\mathbf{r}_{EM\parallel}|^2$ are the bending, stretching and spring energy, respectively. Here $\delta\mathbf{r}_{EM\perp}$ and $\delta\mathbf{r}_{EM\parallel}$ are the transverse and parallel components of $\delta\mathbf{r}_{EM}$ with respect to the polymer. Minimizing the total energy $E_{EM} = \Delta H_{EM} - \mathbf{F} \cdot \delta\mathbf{r}_{EM}$, where $\mathbf{F} \cdot \delta\mathbf{r}_{EM}$ stands for the work, we obtain the displacement

$$\begin{aligned}
 \delta\mathbf{r}_{EM\parallel} &= \frac{\mathbf{F}_\parallel}{2\mu/\ell_c + K_{\parallel}} \\
 \delta\mathbf{r}_{EM\perp} &= \frac{\mathbf{F}_\perp}{6\kappa/\ell_c^3 + K_{\perp}},
 \end{aligned} \tag{S3}$$

where \mathbf{F}_\perp and \mathbf{F}_\parallel are the transverse and parallel components of \mathbf{F} respect to the polymer.

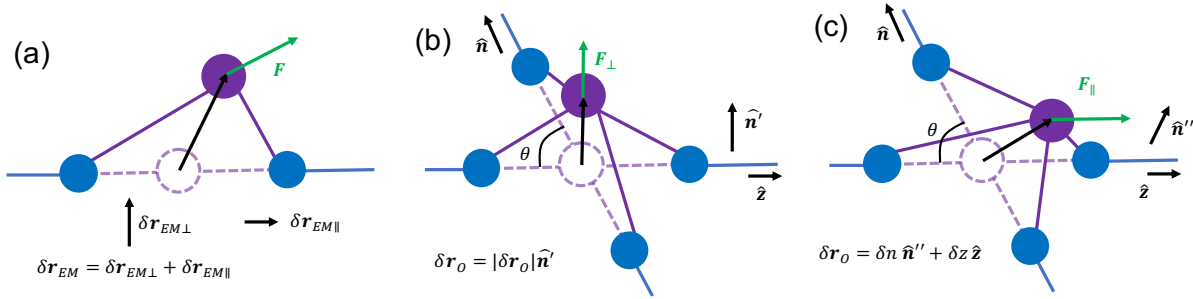


Figure S1. Illustration of the test force approach. The displacement of a crosslinker in the EMN due to a test force \mathbf{F} (a), the displacement of a crosslinker in the original network due to a perpendicular test force \mathbf{F}_\perp (b) and, the displacement of a crosslinker in the original network due to a longitudinal test force \mathbf{F}_\parallel (c).

Next we switch to the original network. In the original network, when a particular crosslinker on one polymer is deformed, the other polymer connected to the crosslinker is deformed at the same time. Without loss of generality, let the orientation of the first polymer be \hat{z} , the orientation of \mathbf{F}_\perp be \hat{x} and the orientation of the second polymer be $\hat{n} = (\sin(\theta)\cos(\phi), \sin(\theta)\sin(\phi), \cos(\theta))$. When the crosslinker is deformed with $\delta\mathbf{r}_O$, the resulting energy is the sum of the bending and stretching energies of two polymers (the bending and stretching energies are written in the discrete forms as in Eq. (S1)):

$$\begin{aligned}\Delta H_O &= \Delta H_b(|\delta\mathbf{r}_O - (\delta\mathbf{r}_O \cdot \hat{z})\hat{z}|) + \Delta H_s(\delta\mathbf{r}_O \cdot \hat{z}) \\ &+ \Delta H_b(|\delta\mathbf{r}_O - (\delta\mathbf{r}_O \cdot \hat{n})\hat{n}|) + \Delta H_s(\delta\mathbf{r}_O \cdot \hat{n})\end{aligned}\quad (\text{S4})$$

The displacement can be found by minimizing the total energy $E_O = \Delta H_O - \mathbf{F} \cdot \delta\mathbf{r}_O$ with respect to $\delta\mathbf{r}_O$. However, an exact solution would be complicated due to coupling of two polymers. We consider a strong stretching limit, $\mu \gg \kappa/\ell_c^2$, which is usually true for semiflexible biopolymers. In this case, the stretching modulus is large enough that the polymers tend to avoid stretching deformations. Therefore, in the following calculation we only keep the leading term in $\kappa/(\mu\ell_c^2)$. To further simplify the calculation we decompose the force \mathbf{F} into \mathbf{F}_\perp and \mathbf{F}_\parallel (transverse and parallel components with respect to the polymer orientation), and calculate their resulting displacements individually. Here we define the displacement caused by \mathbf{F}_\perp as $\delta\mathbf{r}_{O\perp}$ and the displacement caused by \mathbf{F}_\parallel as $\delta\mathbf{r}_{O\parallel}$ (note that $\delta\mathbf{r}_{O\perp}$ and $\delta\mathbf{r}_{O\parallel}$ may not be perpendicular or parallel to the polymer orientation). In the linear regime, the displacements caused by \mathbf{F}_\perp and \mathbf{F}_\parallel should be additive, *i.e.*, $\delta\mathbf{r}_O = \delta\mathbf{r}_{O\perp} + \delta\mathbf{r}_{O\parallel}$.

Let us start with \mathbf{F}_\perp and consider the resulting displacement $\delta\mathbf{r}_{O\perp}$. By definition, the transverse displacement can be aligned in any direction that is perpendicular to \hat{z} . However, to avoid stretching deformation, the only possible direction of $\delta\mathbf{r}_{O\perp}$ is the direction \hat{n}' that is perpendicular to both \hat{z} and \hat{n} , $\hat{n}' = (\sin(\phi), -\cos(\phi), 0)$, see Fig. S1 (b). Assuming $\delta\mathbf{r}_{O\perp} = |\delta\mathbf{r}_{O\perp}|\hat{n}'$, we have $\Delta H_O = (6\kappa/\ell_c^3)|\delta\mathbf{r}_{O\perp}|^2$, and

$$\delta\mathbf{r}_{O\perp} = \frac{|\mathbf{F}_\perp|\sin(\phi)\hat{n}'}{12\kappa/\ell_c^3}\quad (\text{S5})$$

We then exert a parallel force \mathbf{F}_\parallel to find $\delta\mathbf{r}_\parallel$. Because the the parallel displacement of the crosslinker must be associated with stretching deformations, we cannot neglect stretching deformations in this case. Since the parallel displacement is determined by \mathbf{F}_\parallel which aligns in \hat{z} direction, $\delta\mathbf{r}_\parallel$ has to align in $\hat{n} - \hat{z}$ plane. Let $\delta\mathbf{r}_\parallel = \delta z\hat{z} + \delta n\hat{n}''$, where $\hat{n}'' = (\cos(\phi), \sin(\phi), 0)$, together with \hat{z} , forms a set of orthogonal bases of $\hat{n} - \hat{z}$ plane, see Fig. S1 (c). Substituting the displacement in Eq. (S4) gives

$$\Delta H_O = \frac{\mu}{\ell_c}\delta z^2 + \frac{\mu}{\ell_c}(\delta z\cos(\theta) + \delta n\sin(\theta))^2 + \frac{3\kappa}{\ell_c^3}\delta n^2 + \frac{3\kappa}{\ell_c^3}(\delta n\cos(\theta) - \delta z\sin(\theta))^2\quad (\text{S6})$$

Minimizing the total energy $E_O = \Delta H_O - |\mathbf{F}_\parallel|\delta z$ with respect to both δz and δn leads to

$$\delta\mathbf{r}_{O\parallel} = \delta z\hat{z} + \delta n\hat{n}'' = \frac{\mathbf{F}_\parallel}{2\mu/\ell_c + 6\kappa/\ell_c^3[\cot(\theta)^2 + 1/\sin(\theta)^2]} + |\mathbf{F}_\parallel|g(\theta)\hat{n}''.\quad (\text{S7})$$

In the first term of Eq. (S7) we only keep the leading term of $\kappa/(\mu\ell_c^2)$ in the denominator. $g(\theta)$ is some function of θ , whose exact form is not important because the second term disappears after taking average over \hat{n} .

To account for the randomness in the crosslinking angle \hat{n} , we take an average over the displacements in Eqs. (S5,S7) with respect to \hat{n} , which gives (again keeping the leading term of $\kappa/(\mu\ell_c^2)$ in the denominator)

$$\begin{aligned}\langle\delta\mathbf{r}_{O\parallel}\rangle_{\hat{n}} &= \frac{\mathbf{F}_\parallel}{2\mu/\ell_c + 18\kappa/\ell_c^3} \\ \langle\delta\mathbf{r}_{O\perp}\rangle_{\hat{n}} &= \frac{\mathbf{F}_\perp}{24\kappa/\ell_c^3},\end{aligned}\quad (\text{S8})$$

Here, the averages are defined by

$$\langle X \rangle_{\hat{n}} = \int d\hat{n} \cdot \mathbf{P}(\hat{n})X,\quad (\text{S9})$$

where $\mathbf{P}(\hat{n})$ is the probability distribution of the orientation \hat{n} . For the spherical coordinate used above we have

$$\langle X \rangle_{\hat{n}} = \int_0^\pi d\theta \int_0^{2\pi} d\phi P(\theta)P(\phi)X,\quad (\text{S10})$$

with $P(\theta) = (2/\pi) \sin^2(\theta)$ and $P(\phi) = 1/(2\pi)$ being the distribution of angles θ and ϕ . Note that although $P(\theta)$ shows a quadratic dependence on $\sin\theta$, it does reflect the distribution of the crosslinking angle θ in an isotropic network: one $\sin(\theta)$ factor comes from the spherical coordinate, the other originates from the fact two polymers are more likely to be crosslinked with large crosslinking angle [1]. For example, two parallel polymers ($\theta = 0$) never crosslink, suggesting that the distribution of $\hat{\mathbf{n}}$ is not isotropic. However, this ‘anisotropic’ distribution of $\hat{\mathbf{n}}$ is because we fix the orientation of the first polymer to be $\hat{\mathbf{z}}$, while the distribution of the orientations of all polymers is still isotropic.

Equating Eq. (S8) to Eq. (S3) gives the two spring constants:

$$\begin{aligned} K_{\parallel} &= \frac{18\kappa}{\ell_c^3} \\ K_{\perp} &= \frac{18\kappa}{\ell_c^3}. \end{aligned} \quad (\text{S11})$$

Equation (S11) describes the effective medium rigidity of 3D networks with monodispersed crosslinking distance ℓ_c . For networks with a distribution of ℓ_c , $P(\ell_c)$, we can repeat the above calculation with an average of Eqs. (S8, S3) with respect to $P(\ell_c)$, leading to

$$\begin{aligned} K_{\parallel} &= \frac{18\kappa}{\langle \ell_c^3 \rangle} \\ K_{\perp} &= \frac{18\kappa}{\langle \ell_c^3 \rangle}. \end{aligned} \quad (\text{S12})$$

Note that above calculation is for 3D networks only. In 2D networks the rigidity is different because of the ‘floppy-mode’ deformation, see Sec. IV for details.

B. Relation to Coherent Potential Approximation (CPA)

The coherent potential approximation (CPA) was first proposed in the context of condensed matter physics [2] and later applied on the classic effective medium theory of 2D lattice-based networks [3]. The basic idea of this technique is that to find an effective medium for a disordered material, one need to find the green functions, $\underline{\mathcal{G}}_O$ and $\underline{\mathcal{G}}_{EM}$, for the material and the effective medium, respectively. The effective medium is then determined by letting $\langle \underline{\mathcal{G}}_O \rangle = \underline{\mathcal{G}}_{EM}$, where the bracket is average over disorder realizations. This method is essentially equivalent to our derivation in Sec. IA as we show below.

For our networks we can define green functions, $\underline{\mathcal{G}}_O(\alpha, \beta, i, j)$ and $\underline{\mathcal{G}}_{EM}(\alpha, \beta, i, j)$, for the original network and the EMN, respectively. Each green function describes the responding displacement of crosslinker i on polymer α due to a force exerted on crosslinker j on polymer β . Assuming the crosslinker displacements are localized, we have

$$\begin{aligned} \underline{\mathcal{G}}_O(\alpha, \beta, i, j) &= \frac{\partial \delta \mathbf{r}_O}{\partial \mathbf{F}} \delta_{\alpha\beta} \delta_{ij} \\ \underline{\mathcal{G}}_{EM}(\alpha, \beta, i, j) &= \frac{\partial \delta \mathbf{r}_{EM}}{\partial \mathbf{F}} \delta_{\alpha\beta} \delta_{ij}. \end{aligned} \quad (\text{S13})$$

Therefore, our requirement that $\langle \delta \mathbf{r}_O \rangle_{\hat{\mathbf{n}}} = \delta \mathbf{r}_{EM}$ naturally leads to $\langle \underline{\mathcal{G}}_O \rangle = \underline{\mathcal{G}}_{EM}$, suggesting that our approach is a CPA.

II. RELATION BETWEEN THE MACROSCOPIC AND MICROSCOPIC DEFORMATIONS

A. The original network

In this section we derive the coefficient tensor $\underline{\underline{\mathbf{T}}}^\alpha$, which relates the macroscopic ($\underline{\underline{\mathbf{\Lambda}}}_O$) and microscopic (\mathbf{u}^α) deformations of the original network via the following equation (Eq. (7) of the main text):

$$\underline{\underline{\mathbf{\Lambda}}}_O = \sum_{\alpha} \int ds \mathbf{u}^\alpha(s) \cdot \underline{\underline{\mathbf{T}}}^\alpha(s), \quad (\text{S14})$$

Here $\underline{\underline{T}}^\alpha(s)$ is a third-order coefficient tensor, which is a function of s . Because the network is assumed to be homogeneous on large scale, the polymers are equal to each other except for their individual orientations. In this case, $\underline{\underline{T}}^\alpha(s) = \underline{\underline{T}}(\hat{\mathbf{n}}^\alpha, s)$, where $\hat{\mathbf{n}}^\alpha$ is the orientation of the α -th polymer. We also assume the network to be isotropic on large scale, such that it does not have any particular direction. Therefore, the only vector that can be used to construct $\underline{\underline{T}}$ is $\hat{\mathbf{n}}$. There are only three possible third-order tensor that can be constructed from $\hat{\mathbf{n}}$: $\hat{\mathbf{n}}\underline{\underline{I}}$, $\underline{\underline{I}}\hat{\mathbf{n}}$ and $\hat{\mathbf{n}}\hat{\mathbf{n}}\hat{\mathbf{n}}$, and $\underline{\underline{T}}$ must be a linear combination of the three tensors:

$$\underline{\underline{T}}(\hat{\mathbf{n}}, s) = a(s)\hat{\mathbf{n}}\hat{\mathbf{n}}\hat{\mathbf{n}} + b(s)\underline{\underline{I}}\hat{\mathbf{n}} + c(s)\hat{\mathbf{n}}\underline{\underline{I}} \quad (\text{S15})$$

with $a(s)$, $b(s)$ and $c(s)$ being coefficients that depends on the position s .

Our goal is to determine the values of a , b and c , such that the relation between $\underline{\underline{\Lambda}}_O$ and \mathbf{u}^α can be obtained by substituting Eq. (S15) into Eq. (S14). To do so we use the only deformation of which the macroscopic-microscopic relation is clear, the affine deformation $\mathbf{u}^\alpha(s) = s\underline{\underline{\Lambda}}_O \cdot \hat{\mathbf{n}}^\alpha$. Because Eq. (S14) holds for arbitrary deformation, the affine deformation must also satisfy Eq. (S14), leading to

$$\begin{aligned} \underline{\underline{\Lambda}}_O &= \sum_\alpha \int ds \left[a(s)s \left[(\underline{\underline{\Lambda}}_O \cdot \hat{\mathbf{n}}^\alpha) \cdot \hat{\mathbf{n}}^\alpha \right] \hat{\mathbf{n}}^\alpha \hat{\mathbf{n}}^\alpha + b(s)s (\underline{\underline{\Lambda}}_O \cdot \hat{\mathbf{n}}^\alpha) \hat{\mathbf{n}}^\alpha + c(s)s \left[(\underline{\underline{\Lambda}}_O \cdot \hat{\mathbf{n}}^\alpha) \cdot \hat{\mathbf{n}}^\alpha \right] \underline{\underline{I}} \right] \\ &= A \left\langle \left[(\underline{\underline{\Lambda}}_O \cdot \hat{\mathbf{n}}) \cdot \hat{\mathbf{n}} \right] \hat{\mathbf{n}} \hat{\mathbf{n}} \right\rangle_{\hat{\mathbf{n}}} + B \left\langle (\underline{\underline{\Lambda}}_O \cdot \hat{\mathbf{n}}) \hat{\mathbf{n}} \right\rangle_{\hat{\mathbf{n}}} + C \left\langle \left[(\underline{\underline{\Lambda}}_O \cdot \hat{\mathbf{n}}) \cdot \hat{\mathbf{n}} \right] \underline{\underline{I}} \right\rangle_{\hat{\mathbf{n}}} \end{aligned} \quad (\text{S16})$$

where $\{A, B, C\} = N \int ds \{a(s), b(s), c(s)\} s$. In the second equality we have replaced the summation with an integral in the large N limit, with $\langle X \rangle_{\hat{\mathbf{n}}}$ being defined in Eq. (S9). This average can be found by writing $\hat{\mathbf{n}}$ in spherical coordinate $\hat{\mathbf{n}} = (\sin(\theta) \cos(\phi), \sin(\theta) \sin(\phi), \cos(\theta))$ and using Eq. (S10), but with an isotropic distribution of $\hat{\mathbf{n}}$: $P(\theta) = \sin(\theta)/2$ and $P(\phi) = 1/(2\pi)$ (note that unlike Sec. I, θ here is not related to a crosslinking angle).

Because Eq. (S16) should be true for arbitrary deformation tensor $\underline{\underline{\Lambda}}_O$, substituting several specific $\underline{\underline{\Lambda}}_O$ into Eq. (S16) is sufficient to determine the values of A , B and C . For a bulk expansion $\underline{\underline{\Lambda}}_O = \gamma \underline{\underline{I}}$, its $\hat{\mathbf{x}}\hat{\mathbf{x}}$ component gives $A/3 + B/3 + C = 1$. For a uniaxial deformation in $\hat{\mathbf{x}}$, $\underline{\underline{\Lambda}}_O = \gamma \hat{\mathbf{x}}\hat{\mathbf{x}}$, the $\hat{\mathbf{x}}\hat{\mathbf{x}}$ component of Eq. (S16) gives $A/5 + B/3 + C/3 = 1$, while its $\hat{\mathbf{y}}\hat{\mathbf{y}}$ component gives $A/15 + C/3 = 0$. Solving the above three constraints leads to

$$\begin{aligned} A &= C = 0 \\ B &= 3 \end{aligned} \quad (\text{S17})$$

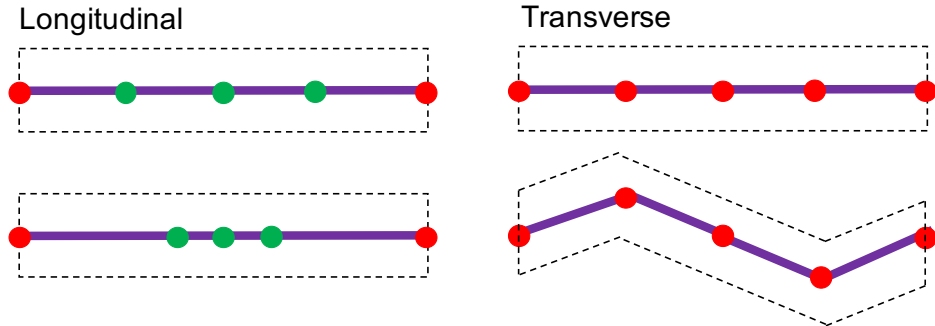


Figure S2. Illustration of the longitudinal and transverse displacements. We embed a single polymer in a box, whose shape stands for the macroscopic deformation of the network. For longitudinal displacements (left), the macroscopic deformation is irrelevant to the displacements of all internal points (green dots), and is only determined by the displacements of two ends (red dots). For transverse displacements (right), macroscopic deformation is affected by the displacements of all points.

In addition to the values of A , B and C , one also needs the dependences of $a(s)$, $b(s)$ and $c(s)$ on s to determine these three functions. Such dependences can be found by examining the geometric properties of a single polymer. Let us use Eqs. (S14,S15) to calculate the resulting deformation tensor of a test displacement $\mathbf{u}(s) = (\mathbf{u}_\perp + \mathbf{u}_\parallel)\delta(s - s_0)$ on one polymer at arbitrary position s_0 , where \mathbf{u}_\perp and \mathbf{u}_\parallel are the transverse and longitudinal components of \mathbf{u} with respect to $\hat{\mathbf{n}}$:

$$\underline{\underline{\Lambda}}_O = (a(s_0) + b(s_0))(\mathbf{u}_\parallel \cdot \hat{\mathbf{n}})\hat{\mathbf{n}}\hat{\mathbf{n}} + b(s_0)\mathbf{u}_\perp \hat{\mathbf{n}} + c(s_0)(\mathbf{u}_\parallel \cdot \hat{\mathbf{n}})\underline{\underline{I}}. \quad (\text{S18})$$

The first and the last terms in Eq. (S18) correspond to macroscopic uniaxial and bulk expansion due to a microscopic longitudinal displacement \mathbf{u}_{\parallel} . As shown in Fig. S2, longitudinal displacements of all internal nodes do not affect the macroscopic deformation of the network. The only longitudinal displacement that affects the macroscopic strain is the displacement of two polymer ends that changes the polymer length. Writing the above statement in mathematical form, we have

$$(a(s) + b(s)) \sim c(s) \sim (\delta(s - L/2) - \delta(s + L/2)). \quad (\text{S19})$$

We now switch to the second term of Eq. (S18), which corresponds to a macroscopic shear deformation due to a microscopic transverse displacement \mathbf{u}_{\perp} . Unlike the longitudinal displacements, the transverse displacements of all points of the polymer can affect the macroscopic deformation, see Fig. S2. We perform a trial shear deformation: opposite displacements on two points $s = s_1$ and $s = s_1 + d$, $\mathbf{u}(s) = \mathbf{u}_{\perp}(\delta(s - s_1) - \delta(s - s_1 - d))$. Such test displacements lead to a macroscopic deformation tensor according to Eq. (S14):

$$\underline{\underline{\mathbf{A}}}_O = [b(s_1) - b(s_1 + d)]\mathbf{u}_{\perp}\hat{\mathbf{n}} \quad (\text{S20})$$

Because of the translational symmetry on the polymer (assuming both points are far from polymer ends), the resulting macroscopic deformation should be independent of the value of s_1 . This suggests that $b(s) - b(s + d) = g(d)$ for arbitrary s and d . Taking derivatives of both sides with respect to s , we have $b'(s) = \text{constant}$ and

$$b(s) \sim s. \quad (\text{S21})$$

Here we have used the fact that $b(0) = 0$ due to the reflectional symmetry at $s = 0$ (the midpoint of the polymer). Equation (S21) may not be accurate when s is close to the two polymer ends because the translational symmetry no longer holds. For long polymers ($L \gg \ell_c$) such effect can be neglected.

Combining Eqs. (S19, S21, S17), the form of $\underline{\underline{\mathbf{T}}}$ is derived :

$$\underline{\underline{\mathbf{T}}}(\hat{\mathbf{n}}, s) = [f_{\parallel}(s) - f_{\perp}(s)]\hat{\mathbf{n}}\hat{\mathbf{n}}\hat{\mathbf{n}} + f_{\perp}(s)\underline{\underline{\mathbf{I}}}\hat{\mathbf{n}} \quad (\text{S22})$$

where

$$\begin{aligned} f_{\parallel} &= a + b = \frac{3}{NL}[\delta(s - L/2) - \delta(s + L/2)] \\ f_{\perp} &= b = \frac{36}{NL^3}s. \end{aligned} \quad (\text{S23})$$

Above we have discussed the case in which the lengths of all polymers are the same. If the polymer lengths of different polymer varies, *i.e.* the polymer length has a distribution $P(L)$, the derivation above is still valid if we replace the definitions of $\{A, B, C\}$ to

$$\{A, B, C\} = N \left\langle \int_{-L/2}^{L/2} ds \{a(s), b(s), c(s)\} s \right\rangle_L, \quad (\text{S24})$$

where $\langle \dots \rangle_L$ is the average over $P(L)$. Following the same derivation with modified definitions of $\{A, B, C\}$, we find modified functions f_{\parallel} and f_{\perp} :

$$\begin{aligned} f_{\parallel} &= \frac{3}{N\langle L \rangle}[\delta(s - L/2) - \delta(s + L/2)] \\ f_{\perp} &= \frac{36}{N\langle L^3 \rangle}s. \end{aligned} \quad (\text{S25})$$

Repeating the same calculation in 2D gives:

$$\begin{aligned} f_{\parallel} &= \frac{2}{N\langle L \rangle}[\delta(s - L/2) - \delta(s + L/2)] \\ f_{\perp} &= \frac{24}{N\langle L^3 \rangle}s. \end{aligned} \quad (\text{S26})$$

B. The EMN

Having found the macroscopic-microscopic relation for the original network, let us define a similar relation for the EMN with a coefficient tensor $\underline{\underline{\mathbf{T}}}_{\text{EM}}^\alpha$,

$$\underline{\underline{\Lambda}}_{\text{EM}} = \sum_{\alpha} \int ds \mathbf{v}^\alpha(s) \cdot \underline{\underline{\mathbf{T}}}_{\text{EM}}^\alpha(s). \quad (\text{S27})$$

The macroscopic-microscopic relations for the original network and the EMN are linked by Eq. (5b) of the main text, *i.e.*, $\partial\gamma_O/\partial\tilde{\mathbf{u}}_i^\alpha = \partial\gamma_{\text{EM}}/\partial\tilde{\mathbf{v}}_i^\alpha$, where $\tilde{\mathbf{u}}_i^\alpha$ and $\tilde{\mathbf{v}}_i^\alpha$ are the crosslinker displacements in the minimum energy state of the original network and the EMN, respectively. To relate Eq. (5b) of the main text with Eqs. (S14, S27), we take derivatives of the xz component of Eqs. (S14, S27), which gives $\partial\gamma_O/\partial\mathbf{u}$ and $\partial\gamma_{\text{EM}}/\partial\mathbf{v}$. For 3D networks which are well sub-isostatic, we have $\partial\gamma_O/\partial\tilde{\mathbf{u}} = \partial\gamma_O/\partial\mathbf{u}$ and $\partial\gamma_{\text{EM}}/\partial\tilde{\mathbf{v}} = \partial\gamma_{\text{EM}}/\partial\mathbf{v}$. This is because in 3D networks the crosslinker displacements in the minimum energy state are localized, *i.e.*, when one crosslinker is deformed, it does not force other crosslinkers to deform together with it (see discussion of the main text). Therefore, when calculating the resulting macroscopic deformation of the displacement of a single crosslinker ($\partial\gamma_O/\partial\tilde{\mathbf{u}}$), that particular crosslinker would be the only one that contributes to the macroscopic deformation. Together with Eq. (5b) of the main text this leads to $\underline{\underline{\mathbf{T}}}_{\text{EM}}^\alpha = \underline{\underline{\mathbf{T}}}^\alpha$ and

$$\underline{\underline{\Lambda}}_{\text{EM}} = \sum_{\alpha} \int ds \mathbf{v}^\alpha(s) \cdot \underline{\underline{\mathbf{T}}}^\alpha(s). \quad (\text{S28})$$

For 2D networks $\underline{\underline{\mathbf{T}}}_{\text{EM}}$ becomes more complicated. While we still have $\partial\gamma_{\text{EM}}/\partial\tilde{\mathbf{v}} = \partial\gamma_{\text{EM}}/\partial\mathbf{v}$ (all polymers can deform independently in the EMN), $\partial\gamma_O/\partial\tilde{\mathbf{u}} \neq \partial\gamma_O/\partial\mathbf{u}$ because the crosslinkers are forced to deform in *floppy modes* [1, 4]. We will detail the calculation of 2D networks in Sec. IV.

III. LINEAR ELASTICITY OF 3D NETWORKS

A. 3D Athermal Networks

In this section we calculate the linear elasticity of 3D athermal networks. The idea is to construct an effective medium network, calculate its effective medium elasticity G_{EM} , and use G_{EM} to approximate the original elasticity G_O . To find G_{EM} , first we need to find the minimum-energy state under an external stress tensor $\underline{\underline{\boldsymbol{\sigma}}}_{\text{EM}}$, *i.e.* minimizing the total energy

$$E_{\text{EM}} = H_{\text{EM}}(\{\mathbf{v}^\alpha(s)\}) - V \underline{\underline{\boldsymbol{\sigma}}}_{\text{EM}} : \underline{\underline{\Lambda}}_{\text{EM}} \quad (\text{S29})$$

where the H_{EM} is defined in Eq. (2) of the main text and V is the network volume. For simplicity we set $V = 1$ hereafter. Without loss of generality we assume the resulting deformation is a simple shear of the xz plane in the \hat{x} direction,

$$\underline{\underline{\Lambda}}_{\text{EM}} = \begin{pmatrix} 0 & 0 & \gamma_{\text{EM}} \\ 0 & 0 & 0 \\ 0 & 0 & 0 \end{pmatrix}. \quad (\text{S30})$$

In the linear regime, the corresponding stress tensor is also limited in the xz direction:

$$\underline{\underline{\boldsymbol{\sigma}}}_{\text{EM}} = \begin{pmatrix} 0 & 0 & \sigma_{\text{EM}} \\ 0 & 0 & 0 \\ \sigma_{\text{EM}} & 0 & 0 \end{pmatrix}. \quad (\text{S31})$$

With Eqs. (S30,S31), we rewrite Eq. (S29) as

$$E_{\text{EM}} = H_{\text{EM}}(\{\mathbf{v}^\alpha(s)\}) - \sigma_{\text{EM}}\gamma_{\text{EM}}, \quad (\text{S32})$$

According to Eq. (S28), the shear strain γ_{EM} , which is the xz component of the deformation tensor, is related to the microscopic deformations via

$$\gamma_{\text{EM}} = \sum_{\alpha} \int ds \mathbf{v}^{\alpha}(s) \cdot \left[\underline{\underline{\mathbf{T}}}^{\alpha}(s) : \hat{\mathbf{x}}\hat{\mathbf{z}} \right], \quad (\text{S33})$$

where the form of $\underline{\underline{\mathbf{T}}}$ is derived in Eq. (S22). To simplify the calculation, let us define $\mathbf{w}^{\alpha} = \mathbf{v}_{\text{NA}\perp}^{\alpha} + \mathbf{v}_{\parallel}^{\alpha}$ or equivalently $\mathbf{v}^{\alpha} = \mathbf{w}^{\alpha} + \mathbf{v}_{\text{A}\perp}^{\alpha}$. Substituting the later in Eq. (S33), we find

$$\gamma_{\text{EM}} = \sum_{\alpha} \int ds \mathbf{w}^{\alpha}(s) \cdot \left[\underline{\underline{\mathbf{T}}}^{\alpha}(s) : \hat{\mathbf{x}}\hat{\mathbf{z}} \right] + \frac{4}{5}\gamma_{\text{EM}}, \quad (\text{S34})$$

where we use the isotropic distribution of the orientation $\hat{\mathbf{n}}$ (see discussion after Eq. (S16)). Equation (S34) suggests a relation between γ_{EM} and \mathbf{w}^{α} :

$$\begin{aligned} \gamma_{\text{EM}} &= \sum_{\alpha} \int ds \mathbf{t}^{\alpha} \cdot \mathbf{w}^{\alpha} \\ &= \sum_{\alpha} \int ds \mathbf{t}_{\parallel}^{\alpha} \cdot \mathbf{w}_{\parallel}^{\alpha} + \sum_{\alpha} \int ds \mathbf{t}_{\perp}^{\alpha} \cdot \mathbf{w}_{\perp}^{\alpha}, \end{aligned} \quad (\text{S35})$$

where $\mathbf{t}^{\alpha} \equiv 5\underline{\underline{\mathbf{T}}}^{\alpha} : (\hat{\mathbf{x}}\hat{\mathbf{z}}) = \mathbf{t}_{\parallel}^{\alpha} + \mathbf{t}_{\perp}^{\alpha}$, with $\mathbf{t}_{\parallel}^{\alpha} = 5f_{\parallel}n_x^{\alpha}n_z^{\alpha}\hat{\mathbf{n}}^{\alpha}$ and $\mathbf{t}_{\perp}^{\alpha} = 5f_{\perp}(n_z^{\alpha}\hat{\mathbf{x}} - n_x^{\alpha}n_z^{\alpha}\hat{\mathbf{n}}^{\alpha})$ being the parallel and transverse components with respect to $\hat{\mathbf{n}}^{\alpha}$. H_{EM} of Eq. (2) of the main text is also rewritten in terms of \mathbf{w}^{α} :

$$H_{\text{EM}} = \sum_{\alpha} \int ds \left[\frac{\kappa}{2} \left| \frac{\partial^2 \mathbf{w}_{\perp}^{\alpha}}{\partial s^2} \right|^2 + \frac{\mu}{2} \left| \frac{\partial \mathbf{w}_{\parallel}^{\alpha}}{\partial s} \right|^2 + \frac{K_{\perp}}{2\ell_c} |\mathbf{w}_{\perp}^{\alpha}|^2 + \frac{K_{\parallel}}{2\ell_c} \left| \mathbf{w}_{\parallel}^{\alpha} - s\gamma_{\text{EM}}n_x^{\alpha}n_z^{\alpha}\hat{\mathbf{n}}^{\alpha} \right|^2 \right] \quad (\text{S36})$$

Note that in Eq. (S36) we have replaced the summation over crosslinkers with an integral. This approximation of the continuum limit is valid when $L \gg \ell_c$, which is usually true for biopolymer networks. The minimum-energy state is defined as the state in which $\delta E_{\text{EM}}/\delta \mathbf{w}^{\alpha} = 0$, which is equivalent to

$$\begin{aligned} \frac{\delta H_{\text{EM}}}{\delta \mathbf{w}_{\perp}^{\alpha}} &= \sigma_{\text{EM}} \frac{\delta \gamma_{\text{EM}}}{\delta \mathbf{w}_{\perp}^{\alpha}}, \\ \frac{\delta H_{\text{EM}}}{\delta \mathbf{w}_{\parallel}^{\alpha}} &= \sigma_{\text{EM}} \frac{\delta \gamma_{\text{EM}}}{\delta \mathbf{w}_{\parallel}^{\alpha}}. \end{aligned} \quad (\text{S37})$$

Substituting Eqs. (S35, S36) into Eq. (S37) leads to the following differential equations

$$\begin{aligned} \kappa \frac{d^4 \mathbf{w}_{\perp}^{\alpha}}{ds^4} + \frac{K_{\perp}}{\ell_c} \mathbf{w}_{\perp}^{\alpha} &= \sigma_{\text{EM}} \mathbf{t}_{\perp}^{\alpha} \\ \mu \frac{d^2 \mathbf{w}_{\parallel}^{\alpha}}{ds^2} + \frac{K_{\parallel}}{\ell_c} (\mathbf{w}_{\parallel}^{\alpha} - \gamma_{\text{EM}} s n_x^{\alpha} n_z^{\alpha} \hat{\mathbf{n}}^{\alpha}) &= \sigma_{\text{EM}} \mathbf{t}_{\parallel}^{\alpha}, \end{aligned} \quad (\text{S38})$$

together with natural boundary conditions (assuming the boundary points are free to move, *i.e.*, $\delta \mathbf{w}$ can take any value at the boundaries)

$$\begin{aligned} \frac{d^2 \mathbf{w}_{\perp}^{\alpha}}{ds^2} = \frac{d^3 \mathbf{w}_{\perp}^{\alpha}}{ds^3} &= 0 & (s = \pm L/2) \\ \frac{d \mathbf{w}_{\parallel}^{\alpha}}{ds} &= \frac{15\sigma_{\text{EM}} n_x^{\alpha} n_z^{\alpha} \hat{\mathbf{n}}^{\alpha}}{N\langle L \rangle \mu} & (s = \pm L/2). \end{aligned} \quad (\text{S39})$$

In the second equation of Eq. (S39) we have integrated the second equation of Eq. (S38) around the boundaries. The solution of Eqs. (S38, S39) is

$$\begin{aligned} \mathbf{w}_{\perp}^{\alpha} &= \frac{10\ell_c^4 \sigma_{\text{EM}} s}{N\langle L^3 \rangle \kappa} (n_z^{\alpha} \hat{\mathbf{x}} - n_x^{\alpha} n_z^{\alpha} \hat{\mathbf{n}}^{\alpha}) \\ \mathbf{w}_{\parallel}^{\alpha} &= \left[\gamma_{\text{EM}} s + \left(\frac{15\sigma_{\text{EM}}}{N\langle L \rangle} - \mu \gamma_{\text{EM}} \right) \cdot \frac{\sinh(\epsilon s)}{\epsilon \mu \cosh(\epsilon L/2)} \right] n_x^{\alpha} n_z^{\alpha} \hat{\mathbf{n}}^{\alpha}. \end{aligned} \quad (\text{S40})$$

Here $\epsilon = 3\sqrt{2}/\lambda_{\text{NA}}$ with $\lambda_{\text{NA}} = \ell_c^2/\sqrt{\kappa/\mu}$ being a characteristic length of non-affine deformation. In Eq. (S40) we have used Eq. (S25) as the values of f_{\parallel} and f_{\perp} and Eq. (S11). Substituting the solution of Eq. (S40) back into Eq. (S35) gives:

$$\gamma_{\text{EM}} = \sigma_{\text{EM}} \left(\frac{15}{N\mu\langle L \rangle} + \frac{20\ell_c^4\epsilon\langle L \rangle}{N\langle L^3 \rangle\kappa\langle \tanh(\epsilon L/2) \rangle} \right). \quad (\text{S41})$$

The shear elasticity, defined as $G_O = G_{\text{EM}} = \sigma_{\text{EM}}/\gamma_{\text{EM}}$, is

$$\frac{G_O}{G_A} = \left[1 + \frac{4\sqrt{2}\lambda_{\text{NA}}\langle L \rangle^2}{\langle L^3 \rangle\langle \tanh(3\sqrt{2}L/2\lambda_{\text{NA}}) \rangle} \right]^{-1}, \quad (\text{S42})$$

where $G_A = \rho\mu/15$ is the affine modulus. Here $\rho = N\langle L \rangle$ is the polymer length density ($V = 1$). Equation (S42) is a general result for any polymer length distribution. For monodispersed networks, *i.e.* $P(L) = \delta(L - \langle L \rangle)$, we have

$$\frac{G_O}{G_A} = \left[1 + \frac{4\sqrt{2}}{(L/\lambda_{\text{NA}})\tanh(3\sqrt{2}L/2\lambda_{\text{NA}})} \right]^{-1} \quad (\text{S43})$$

To compare with the simulation results in Ref. [5], we also consider networks with exponentially distributed polymer length, $P(L) = \exp(-L/\langle L \rangle)/\langle L \rangle$. In this case, we have $\langle L^3 \rangle = 6\langle L \rangle^3$, and

$$\frac{G_O}{G_A} = \left[1 + \frac{2\sqrt{2}\lambda_{\text{NA}}}{3\langle L \rangle/\lambda_{\text{NA}}\langle \tanh(3\sqrt{2}L/2\lambda_{\text{NA}}) \rangle} \right]^{-1} \quad (\text{S44})$$

To examine the importance of K_{\parallel} for the non-affine deformations, we set the value of K_{\parallel} to 0 when solving Eq. (S38), leading to

$$\mathbf{w}_{\parallel}^{\alpha} = \frac{15\sigma_{\text{EM}}}{N\langle L \rangle\mu} s n_x^{\alpha} n_z^{\alpha} \hat{\mathbf{n}}^{\alpha}, \quad (\text{S45})$$

where the solution of \mathbf{w}_{\perp} is as in Eq. (S40). The corresponding G_O for $K_{\parallel} = 0$ is

$$\frac{G_O}{G_A} = \left[1 + \frac{8\lambda_{\text{NA}}^2\langle L \rangle}{3\langle L^3 \rangle} \right]^{-1} \quad (\text{S46})$$

We find that removing K_{\parallel} almost does not change the shear modulus, see Fig. 3 of the main text. The reason for this is that the longitudinal displacement is always restricted by μ , even in the absence of K_{\parallel} . This is different from K_{\perp} , which when setting to 0 results in diverging \mathbf{w}_{\perp} and therefore vanishing G (see Eq. (S40)). Therefore, we conclude that K_{\perp} is crucial for calculating the non-affine deformation while K_{\parallel} is not.

B. 3D Thermal Networks

So far we have found non-affine deformation for athermal networks ($T = 0$), in this section let us consider thermal networks ($T > 0$). The non-zero temperature generates thermal fluctuations of the polymer displacements \mathbf{w}^{α} . Therefore, the network shear deformation γ_{EM} also has thermal fluctuations, and we should therefore define $G_{\text{EM}} = \sigma_{\text{EM}}/\langle \gamma_{\text{EM}} \rangle$, where the bracket stands for average over noise realizations. γ_{EM} is related to \mathbf{w}^{α} via Eq. (S35):

$$\gamma_{\text{EM}} = \frac{15}{N\langle L \rangle} \sum_{\alpha} n_x^{\alpha} n_z^{\alpha} \hat{\mathbf{n}}^{\alpha} \cdot \left[\mathbf{w}_{\parallel}^{\alpha}(s = L/2) - \mathbf{w}_{\parallel}^{\alpha}(s = -L/2) \right] + \sum_{\alpha} \int ds t_{\perp}^{\alpha} \cdot \mathbf{w}_{\perp}^{\alpha}, \quad (\text{S47})$$

where we have used values of f_{\parallel} in Eq. (S25). For simplicity hereafter we consider polymers in the inextensible limit ($\mu \rightarrow \infty$), which is appropriate for most biopolymers. In this case the network deformation can be described by only the transverse displacements \mathbf{w}^{α} , while the longitudinal end-to-end distance is related to the transverse displacements via [6]

$$\hat{\mathbf{n}}^{\alpha} \cdot \left[\mathbf{w}_{\parallel}^{\alpha}(s = L/2) - \mathbf{w}_{\parallel}^{\alpha}(s = -L/2) \right] = L_0 - \frac{1}{2} \int ds \left| \frac{\partial \mathbf{w}_{\perp}^{\alpha}}{\partial s} \right|^2, \quad (\text{S48})$$

with $\ell_p = \kappa/k_B T$ being the persistence length. Here L_0 is the contaction of the end-to-end distance without external stress, which will later be defined in Eq. (S54).

For inextensible polymers with $K_{\parallel} = 0$ (here K_{\parallel} is set to 0 for simplicity, since it only slightly affects the non-affinity of athermal networks, see discussion after Eq. (S46)), the network Hamiltonian is (see Eq. (S36))

$$H_{\text{EM}} = \sum_{\alpha} \int ds \left[\frac{\kappa}{2} \left| \frac{\partial^4 \mathbf{w}_{\perp}^{\alpha}}{\partial s^4} \right|^2 + \frac{K_{\perp}}{2\ell_c} |\mathbf{w}_{\perp}^{\alpha}|^2 \right]. \quad (\text{S49})$$

Because the Hamiltonian is quadratic, the thermal average $\langle \mathbf{w}_{\perp}^{\alpha} \rangle$ is same as the minimum-energy solution in Eq. (S40). The fluctuations around the minimum-energy state, $\mathbf{w}_{\perp}^{\alpha} - \langle \mathbf{w}_{\perp}^{\alpha} \rangle$, is expanded into Fourier series:

$$\mathbf{w}_{\perp}^{\alpha} - \langle \mathbf{w}_{\perp}^{\alpha} \rangle = \sum_q \left[w_{1q}^{\alpha} \sin(q(s+L/2)) \hat{\mathbf{n}}_1^{\alpha} + w_{2q}^{\alpha} \sin(q(s+L/2)) \hat{\mathbf{n}}_2^{\alpha} \right], \quad (\text{S50})$$

where $q = m\pi/L$ ($m = 1, 2, 3, \dots$) is the wave number, $\hat{\mathbf{n}}_1^{\alpha}$ and $\hat{\mathbf{n}}_2^{\alpha}$ are two unit vectors perpendicular to both $\hat{\mathbf{n}}^{\alpha}$ and each other, such that $\hat{\mathbf{n}}^{\alpha}$, $\hat{\mathbf{n}}_1^{\alpha}$ and $\hat{\mathbf{n}}_2^{\alpha}$ form a basis of the 3-dimensional space. Substituting Eq. (S50) into Eq. (S48) leads to

$$\left\langle \hat{\mathbf{n}}^{\alpha} \cdot \left[\mathbf{w}_{\parallel}^{\alpha}(s=L/2) - \mathbf{w}_{\parallel}^{\alpha}(s=-L/2) \right] \right\rangle = L_0 - \frac{L}{4} \sum_q q^2 \left[\langle (w_{1q}^{\alpha})^2 \rangle + \langle (w_{2q}^{\alpha})^2 \rangle \right], \quad (\text{S51})$$

where we have neglected the contribution from $\langle \mathbf{w}_{\perp}^{\alpha} \rangle$. This is because $\langle \mathbf{w}_{\perp}^{\alpha} \rangle$ is linear in σ_{EM} , whose leading contribution to Eq. (S51) quadratic in σ_{EM} , hence, it does not contribute to linear elasticity. The thermal fluctuations also perturb the system total energy E_{EM} from its minimum E_{min} . Substituting Eqs. (S47, S51) into Eq. (S32) gives

$$E_{\text{EM}} - E_{\text{min}} = \frac{L}{4} \sum_{mq} (\kappa q^4 + \tau_{\parallel}^{\alpha} q^2 + \frac{K_{\perp}}{\ell_c}) [(w_{1q}^{\alpha})^2 + (w_{2q}^{\alpha})^2], \quad (\text{S52})$$

where $\tau_{\parallel}^{\alpha} = 15\sigma_{\text{EM}} n_x^{\alpha} n_z^{\alpha} / (N\langle L \rangle)$ is the effective longitudinal tension on the α -th polymer. The equilibrium amplitudes of the Fourier modes then satisfy the equipartition theorem,

$$\langle (w_{1q}^{\alpha})^2 \rangle = \langle (w_{2q}^{\alpha})^2 \rangle = \frac{2k_B T}{L(\kappa q^4 + \tau_{\parallel}^{\alpha} q^2 + K_{\perp}/\ell_c)}. \quad (\text{S53})$$

Setting $\tau_{\parallel} = 0$ in Eq. (S53) gives the zero-stress amplitudes. Because $\langle \mathbf{w} \rangle$ must be zero in the absence of stress, substituting the zero-stress amplitudes into Eq. (S51) gives

$$L_0 = \sum_q \frac{k_B T q^2}{\kappa q^4 + K_{\perp}/\ell_c}. \quad (\text{S54})$$

Substituting Eqs. (S53, S54) into Eq. (S51), we obtain the average longitudinal displacement

$$\begin{aligned} \left\langle \hat{\mathbf{n}}^{\alpha} \cdot \left[\mathbf{w}_{\parallel}^{\alpha}(s=L/2) - \mathbf{w}_{\parallel}^{\alpha}(s=-L/2) \right] \right\rangle &= \sum_q \left[\frac{k_B T q^2}{\kappa q^4 + K_{\perp}/\ell_c} - \frac{k_B T q^2}{\kappa q^4 + \tau_{\parallel}^{\alpha} q^2 + K_{\perp}/\ell_c} \right] \\ &= \sum_q \frac{k_B T \tau_{\parallel}^{\alpha} q^4}{(\kappa q^4 + K_{\perp}/\ell_c)^2}. \end{aligned} \quad (\text{S55})$$

In the second equation we have used the fact that σ_{EM} is small, thus τ_{\parallel} is also small and expanded to linear order in σ_{EM} . Because $K_{\perp}/\ell_c \sim \kappa/\ell_c^4 \gg \kappa/L^4$, we can replace the summation in Eq. (S55) with an integral, leading to

$$\left\langle \hat{\mathbf{n}}^{\alpha} \cdot \left[\mathbf{w}_{\parallel}^{\alpha}(s=L/2) - \mathbf{w}_{\parallel}^{\alpha}(s=-L/2) \right] \right\rangle \simeq 0.01 \frac{L \ell_c^3 k_B T}{\kappa^2} \tau_{\parallel}^{\alpha} = \frac{L \tau_{\parallel}^{\alpha}}{\mu_{\text{ph}}}, \quad (\text{S56})$$

where $\mu_{\text{ph}} \simeq 100\kappa\ell_p/\ell_c^3$ is the effective stretch rigidity of a phantom chain, which is later discussed in Sec. III C. We then calculate the network shear deformation by substituting Eq. (S56) and the solution of $\langle \mathbf{w}_{\perp}^{\alpha} \rangle$ (Eq. (S40)) into Eq. (S47):

$$\langle \gamma_{\text{EM}} \rangle = \frac{40\ell_c^4 \sigma_{\text{EM}}}{N\langle L^3 \rangle \kappa} + \frac{15\sigma_{\text{EM}}}{N\langle L \rangle \mu_{\text{ph}}}. \quad (\text{S57})$$

Eq. (S57) gives the shear modulus,

$$G_O = \frac{\rho\mu_{\text{ph}}}{15}(1 + 266.7\ell_c\ell_p\langle L\rangle/\langle L^3\rangle)^{-1}, \quad (\text{S58})$$

which may vary according to different polymer length distributions. For monodispersed networks we have

$$G_O = \frac{\rho\mu_{\text{ph}}}{15}(1 + 266.7\ell_c\ell_p/L^2)^{-1}. \quad (\text{S59})$$

C. High-Molecular-Weight Limit

Above we have calculated the linear elasticity of athermal networks (Sec. III A) and thermal networks (Sec. III B). For both networks we find that the ratio between filament length L and the non-affine length scale λ_{NA} governs non-affinity (Eqs. (S42, S58)). Here $\lambda_{\text{NA}} = \ell_c^2/\sqrt{\kappa/\mu}$ for athermal networks and $\lambda_{\text{NA}} \simeq 16.3\sqrt{\ell_c\ell_p}$ for thermal networks. While for athermal networks G_O reduces to the affine modulus G_A when $L \gg \lambda_{\text{NA}}$, for thermal networks the affine modulus is not achieved for large L . In fact, taking $L \gg \lambda_{\text{NA}}$ in Eq. (S58) we have $G_O = G_{\text{ph}}$, where $G_{\text{ph}} = \rho\mu_{\text{ph}}/15$ is a phantom-network-like limit of our model. Here, $\mu_{\text{ph}} \simeq 100\kappa\ell_p/\ell_c^3$ is the effective stretch rigidity of a phantom chain, which is different by a numerical factor from the affine stretch modulus $\mu_A = 90\kappa\ell_p/\ell_c^3$ [7, 8]. There are two reasons for this difference. The first reason is that in our model the crosslinkers of each polymer are allowed to deform in a non-affine manner, similar to phantom networks for flexible polymers [9]. The second reason is that our model takes into account the bending interactions between adjacent segments, which is not taken into account in the traditional affine model [7, 8]. Interestingly, these two factors changes the effective stretch rigidity in opposite directions: the non-affine deformation of a phantom chain lowers the stretch rigidity, while the inter-segment bending interactions strengthen it. As a result of the combining effect of the above two factors, μ_{ph} is 10% larger than μ_A .

We also need to clarify between two ratios, ℓ_c/L and λ_{NA}/L . Our predicted non-affinity is only significant when $L < \lambda_{\text{NA}}$, and can thus be interpreted as a *finite-length correction* for large λ_{NA}/L values. On the other hand, the assumption $L \gg \ell_c$ is used through, implying that an additional *finite-length correction* should be applied for large ℓ_c/L values. The fact that we take into account one correction while neglecting the other suggests that $\ell_c \ll \lambda_{\text{NA}}$. For athermal networks this leads to $\sqrt{\kappa/\mu} \ll \ell_c$, which is clearly satisfied considering that $\sqrt{\kappa/\mu}$ is of the molecular scale [6]. For thermal networks this results in $\ell_c \ll \ell_p$, which is exactly the definition of semiflexible polymers. Therefore, for both athermal and thermal networks $\ell_c \ll \lambda_{\text{NA}}$ should be naturally satisfied, suggesting that our assumptions are reasonable.

IV. 2D NETWORKS

In the previous section we have calculated the non-affine deformation of 3D networks. In this section we apply the theory on 2D networks and demonstrate the difference between 2D and 3D networks.

For 3D athermal networks we have shown that its linear elasticity is governed by a non-affine length $\lambda_{\text{NA}} = \ell_c^2/\sqrt{\kappa/\mu}$, where in the bend-dominated regime $L \ll \lambda_{\text{NA}}$ we find that $G_O \sim L^2$. Similar non-affine length, together with the scaling dependence in the bend-dominated regime, has also been observed previously in numerical simulations of 2D networks [10–14], although the value of the non-affine length and the scaling exponent may vary with network structure. For any network structure $G_O \sim L^\xi$ in the bend-dominated regime, with $\lambda_{\text{NA}} = \ell_c^{1+2/\xi}(\kappa/\mu)^{-1/\xi}$ [6]. Numerical studies have revealed the scaling exponents ξ in various network structures, which are $\xi = 2$ in 2D lattice-based networks [13, 14] and $\xi = 4$ or 5 in 2D Mikado networks [11, 12]. Although several analytical models has been proposed for some of the above network structures, a unified model which explains how the exponent ξ changes with network structure is lacking. Below we provide an analytical understanding of 2D networks using our EMN approach.

Before we detail the derivation, let us point out an important difference between 2D and 3D networks, which is the Maxwell connectivity for rigidity percolation. Maxwell found that a critical connectivity (isostatic point) for spring networks is $Z = 2d$, where d is the dimension [15]. This suggests that $Z = 4$ in 2D and $Z = 6$ in 3D. If the connectivity exceeds this critical connectivity, a spring network without bending rigidity would be rigid, while subisostatic networks are floppy without bending rigidity. In crosslinked networks, a crosslinker that connects two polymers usually provides a local connectivity of 4 (3 if the crosslinker is near one of the polymer ends). Therefore, 2D networks are very close to their isostatic point, while 3D networks are far from it. As we discuss in the main text, in 3D networks a crosslinker can have a localized displacement, while in 2D networks the displacement must be non-localized. In fact, in 2D networks the total number of independent deformation modes equals to the number of

polymers N [4]. Each of these deformation modes, the so-called ‘floppy modes’, corresponds to the deformation of an entire polymer [1]. Such non-local displacements in 2D networks will affect both the spring constant K_{\perp} and the coefficient tensor $\underline{T}_{\text{EM}}$ in the EMN, as we discuss in detail below.

A. Effective Medium Rigidity in 2D EMN

Because we are interested in the scaling exponent ξ in the bend-dominated regime, for simplicity we assume $\mu \rightarrow \infty$ heretofore. In this case the longitudinal displacements \mathbf{u}_{\parallel} can be neglected, such that the only spring constant that affects the network deformation is K_{\perp} .

We first consider a lattice-based network, *i.e.* with a constant crosslinking length ℓ_c . The Hamiltonians of the original network and the EMN are

$$\begin{aligned} H_O &= \sum_{\alpha} \int ds \frac{\kappa}{2} \left| \frac{\partial^2 \mathbf{u}_{\perp}^{\alpha}}{\partial s^2} \right|^2 \\ H_{\text{EM}} &= \sum_{\alpha} \int ds \left[\frac{\kappa}{2} \left| \frac{\partial^2 \mathbf{v}_{\perp}^{\alpha}}{\partial s^2} \right|^2 + \frac{K_{\perp}}{2\ell_c} |\mathbf{v}_{\perp}^{\alpha}|^2 \right]. \end{aligned} \quad (\text{S60})$$

We follow the same steps as in Sec. I, *i.e.* calculating the resulting displacement $\delta \mathbf{r}$ of a test force \mathbf{F} in both networks. Similar to what we found in Sec. I, in the original network the displacement $\delta \mathbf{r}_O$ of one crosslinker leads to a bending energy $\Delta H_b \sim (\kappa/\ell_c^3) |\delta \mathbf{r}_O|^2$. Following the introductory paragraph and Ref. [1], in 2D networks when one crosslinker is deformed, it must deform an entire polymer together with it, leading to deformation of L/ℓ_c crosslinkers in total. Therefore, we have $\Delta H_O \sim (L/\ell_c)(\kappa/\ell_c^3) |\delta \mathbf{r}_O|^2$, and

$$\delta \mathbf{r}_{O\perp} \sim \frac{\mathbf{F}_{\perp}}{(L/\ell_c)(\kappa/\ell_c^3)}. \quad (\text{S61})$$

The crosslinker displacements in the EMN are localized, unlike the original network. Therefore, $\delta \mathbf{r}_{\text{EM}\perp}$ still follows Eq. (S3). Equating Eq. (S3) with Eq. (S61) gives

$$K_{\perp} \sim \frac{L}{\ell_c} \frac{\kappa}{\ell_c^3}. \quad (\text{S62})$$

In Mikado networks, the crosslinking distance ℓ_c is not a constant, but follows an exponential distribution, $P(\ell_c) = \exp(-\ell_c/\langle \ell_c \rangle)/\langle \ell_c \rangle$. To account for this distribution of ℓ_c , one should modify the bending energy of a single crosslinker to $\Delta H_b \sim \langle \kappa/\ell_c^3 \rangle |\delta \mathbf{r}_O|^2$. Together with the number of crosslinkers on each polymer $L/\langle \ell_c \rangle$, we modify Eq. (S62) to

$$K_{\perp} \sim \frac{L}{\langle \ell_c \rangle} \left\langle \frac{\kappa}{\ell_c^3} \right\rangle, \quad (\text{S63})$$

where the averages are with respect to $P(\ell_c)$. However, the average $\langle \kappa/\ell_c^3 \rangle$ diverges because ℓ_c can be arbitrarily small. To resolve this divergence, we adopt the minimum-cutoff method proposed in Ref. [1]: If the distance between two crosslinkers is smaller than a cutoff distance ℓ_{\min} , we remove the relative bending interactions between them. This is because when two crosslinkers are too close to each other, the energy to cause relative displacement between them is extremely large, such that it is energetically favorable to move the entire connected polymer instead of bending the two crosslinkers. Hence, the cutoff length is defined as

$$\frac{\kappa}{\ell_{\min}^3} = \frac{L}{\langle \ell_c \rangle} \left\langle \frac{\kappa}{\ell_c^3} \right\rangle_{\ell_c > \ell_{\min}}, \quad (\text{S64})$$

where the LHS is effective rigidity to introduce bending between two crosslinkers with distance ℓ_{\min} , and the RHS is the effective rigidity to deform an entire polymer. For $\ell_{\min} \ll \langle \ell_c \rangle$, the average of κ/ℓ_c^3 is dominated by contribution from $\ell_c \sim \ell_{\min}$, in which case it can be approximated by $\kappa/(\ell_{\min}^2 \langle \ell_c \rangle)$. With this approximation, Eq. (S64) gives $\ell_{\min} \sim \langle \ell_c \rangle^2 / L$, and

$$K_{\perp} \sim \frac{\kappa}{\ell_c^6} L^3. \quad (\text{S65})$$

Note that in Eq. (S65) we have used ℓ_c to denote $\langle \ell_c \rangle$.

B. Relate Macroscopic and Microscopic Deformations in 2D EMN

Having found the effective medium rigidity, let us continue by deriving the coefficient tensor which relates the macroscopic and microscopic deformations in 2D EMN. Due to the non-local displacements in 2D networks, the coefficient tensor $\underline{\underline{\mathbf{T}}}_{\text{EM}}$ of 2D EMN differs from $\underline{\underline{\mathbf{T}}}$ of 2D original networks. Following Eq. (S27), in 2D EMN the deformation tensor $\underline{\underline{\mathbf{\Lambda}}}_{\text{EM}}$ is related to the microscopic displacements $\mathbf{v}^\alpha(s)$ via

$$\underline{\underline{\mathbf{\Lambda}}}_{\text{EM}} = \sum_{\alpha} \int ds \mathbf{v}_{\perp}^{\alpha}(s) \cdot \underline{\underline{\mathbf{T}}}_{\text{EM}}^{\alpha}(s), \quad (\text{S66})$$

Note that we have only included the transverse displacements, since μ is assumed to be ∞ which prohibits any longitudinal displacements. Because in 2D there is only one transverse direction, we have $\mathbf{v}_{\perp}^{\alpha}(s) = v^{\alpha}(s) \hat{\mathbf{n}}_{\perp}^{\alpha}$ with $\hat{\mathbf{n}}_{\perp}^{\alpha}$ being the unit vector of the transverse direction of the α -th polymer. Taking the xy component (assuming that is the shear direction) of Eq. (S66) and writing it in a discrete form we have

$$\gamma_{\text{EM}} = \sum_{\alpha i} r_i^{\alpha} v_i^{\alpha}, \quad (\text{S67})$$

where $v_i^{\alpha} = v^{\alpha}(s_i)$ is the displacement of each crosslinker with s_i being the position of the i -th crosslinker, and r_i^{α} is the coefficient.

For the original network, we have (see Eq. (S14))

$$\begin{aligned} \underline{\underline{\mathbf{\Lambda}}}_{\text{O}} &= \sum_{\alpha} \int ds \mathbf{u}_{\perp}^{\alpha}(s) \cdot \underline{\underline{\mathbf{T}}}_{\text{O}}^{\alpha}(s) \\ &= \sum_{\alpha} \int ds f_{\perp}(s) \mathbf{u}_{\perp}^{\alpha}(s) \hat{\mathbf{n}}^{\alpha}, \end{aligned} \quad (\text{S68})$$

where we have used Eq. (S22). We also rewrite the xy component of Eq. (S68) in the discrete version

$$\gamma_{\text{O}} = \sum_{\alpha i} t_i^{\alpha} u_i^{\alpha}, \quad (\text{S69})$$

where $u_i^{\alpha} = \mathbf{u}_{\perp}^{\alpha}(s_i) \cdot \hat{\mathbf{n}}_{\perp}^{\alpha}$ and

$$t_i^{\alpha} = \ell_c f_{\perp}(s_i) \hat{\mathbf{n}}_{\perp}^{\alpha} \hat{\mathbf{n}}^{\alpha} : \hat{\mathbf{x}} \hat{\mathbf{y}}. \quad (\text{S70})$$

We are interested in equating $\partial \gamma_{\text{O}} / \partial \tilde{u}_i^{\alpha}$ to $\partial \gamma_{\text{EM}} / \partial \tilde{v}_i^{\alpha}$, where \tilde{u}_i^{α} and \tilde{v}_i^{α} are crosslinker displacements in the minimum-energy state (see Eq. (5b) of the main text). Because in the minimum-energy state other $M = L/\ell_c - 1$ crosslinkers must deform together with the given crosslinker, we can write

$$\frac{\partial \gamma_{\text{O}}}{\partial \tilde{u}_i^{\alpha}} = t_i^{\alpha} + \sum_{m=1}^M c(\alpha, \alpha_m, i, i_m) t_{i_m}^{\alpha_m}, \quad (\text{S71})$$

where the summation represents the contribution from other crosslinkers in the floppy mode deformation, with the m -th crosslinker of the floppy mode having crosslinker number i_m on the α_m -th polymer number. $c(\alpha, \alpha_m, i, i_m)$ is a dimensionless coefficient which is determined by the crosslinking angle.

In the EMN, on the other hand, the crosslinker displacements are uncorrelated as in 3D, such that

$$\frac{\partial \gamma_{\text{EM}}}{\partial \tilde{v}_i^{\alpha}} = r_i^{\alpha}, \quad (\text{S72})$$

Comparing Eq. (S72) and Eq. (S71) leads to

$$r_i^{\alpha} = t_i^{\alpha} + \sum_{m=1}^M c(\alpha, \alpha_m, i, i_m) t_{i_m}^{\alpha_m} \quad (\text{S73})$$

To write it in a more general way,

$$r_i^{\alpha} \simeq \sum_{\beta j} c(\alpha, \beta, i, j) t_j^{\beta}, \quad (\text{S74})$$

where $c(\alpha, \beta, i, j) \neq 0$ if u_i^{α} and u_j^{β} are in the same floppy mode, and $c(\alpha, \beta, i, j) = 0$ in other cases. Here we have neglected the first term in Eq. (S73) as the summation term dominates when $M \gg 1$.

C. Linear Elasticity in 2D networks

Having obtained both the effective medium rigidity and the coefficient tensor in 2D EMN, we now calculate the linear elasticity of 2D networks. Because in 2D networks K_{\perp} shows linear (lattice) or cubic (Mikado) dependence on L , in the $L \gg \ell_c$ limit we have $K_{\perp} \gg \kappa/\ell_c^3$, such that the spring energy dominates H_{EM} and the bending term in H_{EM} can be neglected (see Eq. (S60)). We then write H_{EM} in the discrete form

$$H_{\text{EM}} \simeq \sum_i^{\alpha} \frac{K_{\perp}}{2} (v_i^{\alpha})^2. \quad (\text{S75})$$

Minimizing the total energy $H_{\text{EM}} - \gamma_{\text{EM}}\sigma_{\text{EM}}$ leads to

$$v_i^{\alpha} = \sigma_{\text{EM}} r_i^{\alpha} / K_{\perp} \quad (\text{S76})$$

Substituting Eq. (S76) back into Eq. (S67) gives

$$\begin{aligned} \gamma_{\text{EM}} &= \frac{\sigma_{\text{EM}}}{K_{\perp}} \sum_{\alpha i} (r_i^{\alpha})^2 \\ &= \frac{\sigma_{\text{EM}}}{K_{\perp}} \sum_{\beta\beta'j'j'} \sum_{\alpha\alpha'ii'} c(\alpha, \beta, i, j) c(\alpha', \beta', i', j') t_j^{\beta} t_{j'}^{\beta'}, \end{aligned} \quad (\text{S77})$$

where we have used Eq. (S74). Because the crosslinking angles are randomly distributed, the coefficient $c(\alpha, \beta, i, j)$ can be regarded as a random variable with zero average and $\langle c(\alpha, \beta, i, j) c(\alpha', \beta', i', j') \rangle = \langle c^2(\alpha, \beta, i, j) \rangle \delta_{\alpha\alpha'} \delta_{\beta\beta'} \delta_{ii'} \delta_{jj'}$. Here $\langle c^2(\alpha, \beta, i, j) \rangle = \bar{c}^2$ if u_i^{α} and u_j^{β} are in the same floppy mode, and zero in other cases. With that we have

$$\sum_{\alpha\alpha'ii'} c(\alpha, \beta, i, j) c(\alpha', \beta', i', j') \simeq M \bar{c}^2 \delta_{\beta\beta'} \delta_{jj'}, \quad (\text{S78})$$

where the number M emerges because there are M other crosslinkers that are in the same floppy mode with crosslinker (β, j) . Substituting Eq. (S78) to Eq. (S77), we have

$$\gamma_{\text{EM}} \sim \frac{\sigma_{\text{EM}} L}{K_{\perp} \ell_c} \sum_{\beta j} (t_j^{\beta})^2. \quad (\text{S79})$$

Substituting Eqs. (S62, S65, S70) into Eq. (S79), together with Eq. (S26) being values of f_{\perp} , we arrive at the non-affine deformation

$$\gamma_{\text{EM}} \sim \begin{cases} \sigma_{\text{EM}} \rho^{-1} \kappa^{-1} \ell_c^4 L^{-2} & (\text{2D, lattice - based}) \\ \sigma_{\text{EM}} \rho^{-1} \kappa^{-1} \ell_c^6 L^{-4} & (\text{2D, Mikado}) \end{cases}, \quad (\text{S80})$$

and also the linear elasticity

$$G_O \approx G_{\text{EM}} \sim \begin{cases} L^2 & (\text{2D, lattice - based}) \\ L^4 & (\text{2D, Mikado}) \end{cases}. \quad (\text{S81})$$

The L^2 dependence of 2D lattice-based networks agree with previous numerical simulations on both random-diluted triangular networks [14] and kagome lattice [13]. For Mikado networks previous numerical simulations have arrived at different conclusions: While Refs. [1, 11] found an exponent close to 4 which agrees with our prediction, Ref. [12] and recent studies on higher molecular weights [16, 17] claim that the exponent is 5. We believe that an important detail in the data processing may be the cause of this disagreement. In Ref. [11] the filament length L (which is equivalent to the polymer length density in their original paper) is modified to $L - L_r$, where $L_r = 5.9\ell_c$ is the rigidity percolation length. This modification tends to correct the finite-length effect of the simulation. However, in Refs [12, 16, 17] such correction is not used. To test whether this correction is the origin of the different observed exponents, we replot the data obtained from Ref. [11, 16, 17], see Fig 4 of the main text. We find that all data collapse on a single curve, which shows $G \sim L^4$ in the bend-dominated regime. This suggests that the exponent 5 is an affair the finite polymer length, and our theoretical prediction of $G \sim L^4$ agrees with multiple numerical simulations.

[1] C. Heussinger and E. Frey, *Phys. Rev. Lett.* **97**, 105501 (2006).

- [2] J. R. Klauder, *Annals of Physics* **14**, 43 (1961).
- [3] S. Feng, M. F. Thorpe, and E. Garboczi, *Phys. Rev. B* **31**, 276 (1985).
- [4] D. Zhou, L. Zhang, and X. Mao, *Phys. Rev. Lett.* **120**, 068003 (2018).
- [5] C. P. Broedersz, M. Sheinman, and F. C. MacKintosh, *Phys. Rev. Lett.* **108**, 078102 (2012).
- [6] C. P. Broedersz and F. C. MacKintosh, *Rev. Mod. Phys.* **86**, 995 (2014).
- [7] F. Gittes and F. C. MacKintosh, *Physical Review E* **58**, R1241 (1998).
- [8] D. C. Morse, *Macromolecules* **31**, 7030 (1998), cited By 177.
- [9] P. J. Flory, *Br. Polym. J.* **17**, 96 (1985).
- [10] D. A. Head, A. J. Levine, and F. C. MacKintosh, *Phys. Rev. Lett.* **91**, 108102 (2003).
- [11] J. Wilhelm and E. Frey, *Phys. Rev. Lett.* **91**, 108103 (2003).
- [12] D. A. Head, A. J. Levine, and F. C. MacKintosh, *Phys. Rev. E* **68**, 061907 (2003).
- [13] X. Mao, O. Stenull, and T. C. Lubensky, *Phys. Rev. E* **87**, 042602 (2013).
- [14] A. J. Licup, A. Sharma, and F. C. MacKintosh, *Phys. Rev. E* **93**, 012407 (2016).
- [15] J. C. M. F.R.S., *The London, Edinburgh, and Dublin Philosophical Magazine and Journal of Science* **27**, 294 (1864).
- [16] A. S. Shahsavari and R. C. Picu, *Int. J. Solids Struct.* **50**, 3332 (2013).
- [17] K. Baumgarten and B. P. Tighe, *Soft Matter* **17**, 10286 (2021).